PERFORMANCE EVALUATION OF SILT FENCE

WITH A SLOPING TOE TRENCH

CHRISTOPHER BRADLEY CROSS
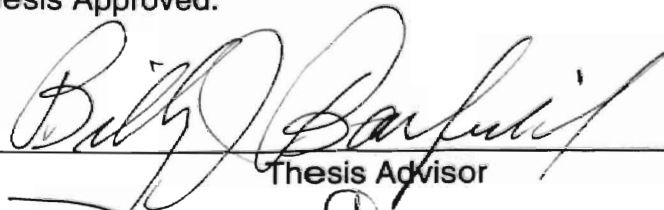
Bachelor of Science

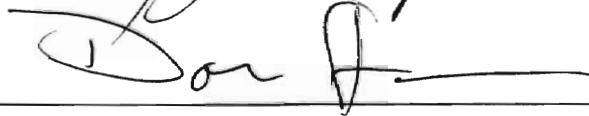Oklahoma State University

Stillwater, Oklahoma

2001

Submitted to the Faculty of the
Graduate College of
Oklahoma State
University
in partial fulfillment of
the requirements for
the Degree of
MASTER OF SCIENCE
August, 2003

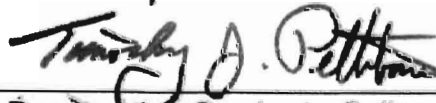# PERFORMANCE EVALUATION OF SILT FENCE

WITH A SLOPING TOE TRENCH

Thesis Approved:

_____
Thesis Advisor

_____

_____

_____
Dean of the Graduate College

ACKNOWLEDGEMENTS

TABLE OF CONTENTS

LIST OF TABLES

LIST OF FIGURES

CHAPTER 1

INTRODUCTION

1.1 Problem Evaluation

Polluted storm water runoff from construction sites frequently flows directly into streets and storm sewer systems, which eventually discharge into surface water impoundments or rivers. The leading pollutant of concern is sediment entrained in construction site storm water according to water quality assessments conducted by the United States Environmental Protection Agency (USEPA, 1998). Sediment loads in runoff from construction sites are typically 10 to 100 times greater than those of agricultural lands, and 1,000 to 10,000 times greater than those of forested areas (Haan et al., 1994). During a short period of time, construction sites can contribute more sediment to streams than can be deposited naturally during several decades. The resulting deposition along with the contribution of other pollutants from construction sites can cause physical, chemical, and biological harm to aquatic ecosystems (USEPA, 1995).

Silt fence is one of many methods available for curtailing sediment-laden runoff from construction areas and has become an integral component of erosion prevention and sediment control plans in most municipalities. In fact, an estimated 23,000 miles of silt fence are sold each year in the United States alone (GMA, 2001). At an approximate cost of six dollars per linear foot for materials and installation (USEPA, 1992), this represents an expenditure of nearly three quarters of a billion dollars for construction activities across the country each year. These installation costs do not account for additional expenses and

1

burdens of maintenance and disposal, which are almost equal to the cost of installation on an annual basis (Brown et al., 1997). Such an investment in a product used to trap sediment on construction sites and to reduce the sediment loads transported and deposited in storm drainage systems and waterways demands scientific evidence to evaluate the actual effectiveness of silt fence. Adequate evidence is not currently available.

A variety of recommended material specifications and installation practices for silt fence have been established by storm water regulating entities, but recommendations are often unenforceable. Formal design considerations are limited and do not account for conditions commonly encountered in construction areas. For example, designs are based on the assumption of silt fence being installed on the contour; however site and equipment limitations typically prevent silt fence from being installed along a contour. Cross contour installation results in significant portions of the fence sloping across contour lines with erosion occurring along the toe trench.

Typical standards and specifications call for the silt fence to be located on mildly sloping areas and to follow the land contour. When silt fence is properly installed under the best possible site conditions, the ends of the silt fence must be sloped upgradient of a contour line such that the silt fence functions as a miniature dam and runoff is not allowed to flow around the edges. Obviously, if the silt fence is undermined, if runoff goes around the edges of the silt fence, or if the silt fence is filled with sediment such that runoff overtops the fence, its effectiveness is significantly reduced.

Field evaluations by Barfield and Hayes (1992, 1999) in South Carolina and Kentucky indicate that actual installations are usually not on the contour but have significant cross contour components that create undercutting problems. While evaluating silt fence installations in Oklahoma, the author found that each site had segments of fence that sloped and each silt fence installation had been undercut to some extent by water flowing along the toe trench. This was due in part to inadequate trench depth and insufficient compaction of backfill material used to secure the fabric. In addition, evidence of overtopping was observed at most of the construction sites. Poor performance of a silt fence is almost certain when it is improperly installed.

Visual inspections of silt fence failures suggest that, in spite of the best installation practices, site limitations often cause flow to concentrate and erode soil at the base of the fabric until undercutting occurs, thus compromising sediment-trapping effectiveness. Alternatively, flow collects at low points along a silt fence and overtops the fabric due to insufficient upslope storage capacity for storm water runoff. A silt fence can actually do more harm than good by adversely altering the impact of sediment-laden runoff in some instances.

Regardless of the reason for installing silt fence across contour lines, a sloping segment of silt fence serves as a diversion instead of functioning as a flow retarding sediment barrier. When overland flow is thus diverted along a silt fence, flow concentrates and erodes the trench backfill material, frequently causing washouts like the one shown in Figure 1.1.

Figure 1.1: Silt fence undermined on a highway construction project near Stillwater, OK

In summary, the final placement of silt fence is routinely determined with inadequate methodology since commonly accepted design specifications assume that silt fence is installed on the contour. Furthermore, silt fences are typically not designed as hydraulic structures to accommodate runoff from a rainfall event of a particular frequency, and failures are often caused by volumes of runoff that exceed the capacity of a silt fence. A lack of design considerations for common situations encountered on construction sites leaves the final design of silt fence in the hands of the person supervising installation operations. There is no replacement for experienced and well-trained installers; however good design specifications and inspection procedures that consider major factors affecting silt fence performance would significantly increase the effectiveness of silt fence and its value as a sediment control practice.

1.2 Objectives of Study

This study is part of a research program aimed at modeling the performance of silt fence using site-specific conditions and fabric characteristics. Acceptable performance of silt fence is defined as the ability to effectively trap sediment on a construction site without experiencing undercutting or overtopping failure. The primary objective of this specific study was to evaluate the hydraulic performance of silt fence and the processes of undercutting for a range of trench slopes and concentrated flow conditions. An additional purpose of this study was to develop a process-based model for predicting the erosion of trench backfill material that occurs when a segment of silt fence functions as a flow diverting structure and converts overland flow into concentrated flow.

CHAPTER 2

LITERATURE REVIEW

2.1 Silt Fence as a Sediment Control Structure

Silt fence, an ubiquitous best management practice (BMP), is used to trap sediment primarily through impounding water and allowing for settling to occur (Haan et al., 1994). Silt fence, like a rock check dam, controls flow through a porous flow control system. The filtering capacity of silt fence (filter fabric) contributes only a small amount of trapping, but serves to make the fence less porous and hence decreases fabric discharge. The amount of trapping in these structures depends on the size of the structure, flow rates into the system, hydraulics of the flow control system, the size distribution of the sediment flowing into the structure, and the chemistry of the sediment-water system (Haan et al., 1994). The following sections will further describe the function, design, and previous studies of silt fence as a temporary sediment control structure.

2.1.1 Description and function. Silt fence is a temporary geotextile barrier designed to retain sediment on construction sites and to reduce sedimentation in down-slope areas. It consists of wood or steel posts with a geotextile filter fabric embedded into the soil and stretched across the posts to which the porous fabric is attached with staples or ties. The primary purpose of silt fence is to retain sediment from small disturbed areas by reducing the velocity of sediment-laden runoff and promoting sediment deposition (Smolen et al., 1998). The fence retains large particle sediment primarily by retarding flow and promoting deposition in the ponded area upslope of the fence (USEPA, 2002).

6

The placement of silt fence is critical to achieve its intended function of collecting and slowly releasing sediment-laden water under overland flow conditions. Silt fence must be properly oriented and installed to curtail sediment-laden runoff from construction areas. In the case of linear construction projects, such as roadways and pipelines, silt fence is used to protect sensitive areas near streams and wetlands. Another common use is along the shoreline of lakes or ponds when construction has disturbed upslope areas. Silt fence may also be used to trap sediment on very small drainage ways with low flows (NRCS, 2000). Silt fence serves no function along ridges or near drainage divides where there is little movement of water. Confining or diverting runoff unnecessarily with a silt fence may create erosion and sedimentation problems that would not otherwise occur, as well as increase construction costs (Barr Engineering Co., 2001).

2.1.2 Design and installation practices. Design specifications and accepted installation practices can vary depending on the regulating entity, but generally accepted requirements are listed below:

- Silt fence fabric is embedded into the soil at a minimum depth of six inches (15 cm).

- Wood or steel support posts are spaced a maximum of 10 feet (3 m) apart and driven securely into the ground at a minimum depth of 1 ft (0.3 m).

- The size of the drainage area is no more than 0.25 acre (1000 m^2) per 100 linear feet (30 m) of silt fence.

- The maximum slope length behind the barrier is 100 feet (30 m), and the maximum gradient upslope of the barrier is 50 percent.

- Under no circumstances should silt fence be constructed in swales or ditch lines where flows are likely to exceed 1 cfs (0.028 cms).

7

According to Richardson and Middlebrooks (1991), silt fence design should be based on three criteria: estimated runoff volume, estimated sediment volume, and geotextile selection. Barfield and Hayes (1999) suggest that the drainage area for a segment of silt fence should be selected based on design storms and local hydrologic conditions so that the silt fence is not expected to overtop during the peak flow from a design storm. Most silt fences should be designed to handle a 10-year, 24-hour design storm and have life expectancy of six months (FHWA, 1998). Hydrologic design for the design storm should result in a silt fence that passes the peak flow without causing damage while also trapping the required amount of sediment (Barfield and Hayes, 1999). To accomplish this design criteria, design aids have been developed for silt fence using computer simulations from the SEDIMOT III model. The design aids yield conservative estimates for silt fence performance as compared to the SEDIMOT III model (Hayes and Barfield, 1995). However, the results from model studies do not account for the impacts of clogging or lateral flow movement on trapping efficiency and therefore give predictions of limited accuracy (USEPA, 2002).

The installation protocol outlined in ASTM D6462 Standard Practices for Silt Fence Installation (ASTM, 2003) provides specific guidance on acceptable installation practices. This practice is applicable to the use of silt fence as a vertical permeable interceptor designed to remove suspended soil from overland, non-concentrated flow. Figure 2.1 illustrates the state-of-the-practice installation protocol for silt fence installed by the traditional trenching method.

Figure 2.1: Standard silt fence installation specifications (NRCS, 2000)
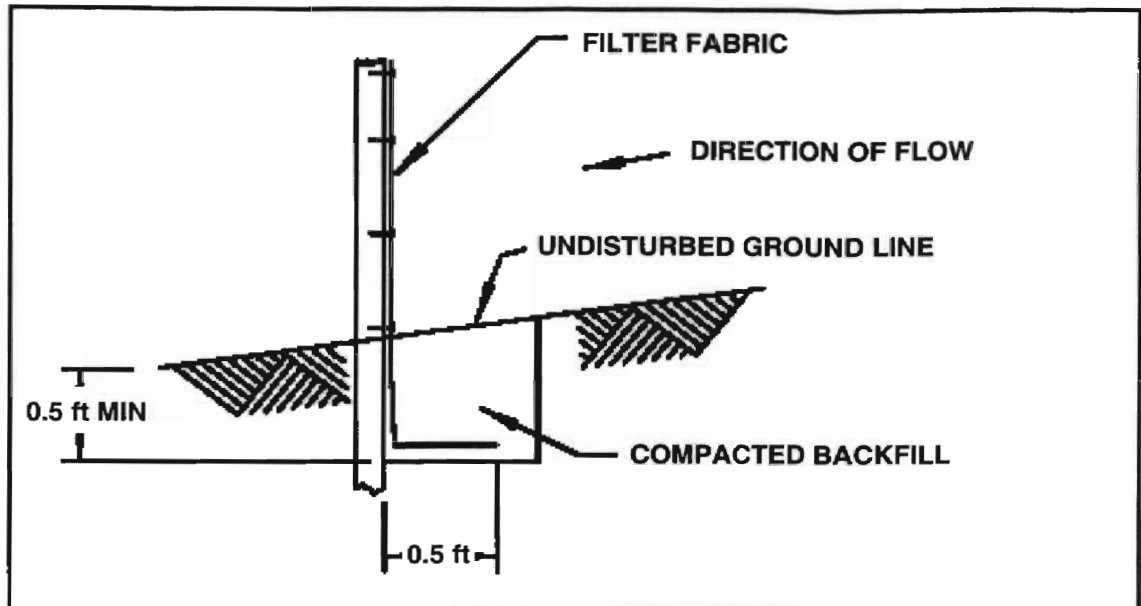
A recent study and proposed revision to ASTM D6462 validates installation of silt fence by the static slicing method, which allows superior compaction at the toe of a silt fence when compared to traditional trench-based methods (CERF, 2001). Static slicing refers to a method of installing silt fence with a knife-like implement instead of using a traditional trench with backfill. CERF (2001) suggests that general installation criteria for silt fence should incorporate the following factors:

- The fabric must have sufficient strength to counter forces created by contained water and sediment.

- The posts must have sufficient strength to counter the forces transferred to them by the fabric.

- The fabric must be installed to ensure that loads are all adequately transferred through the fabric to the posts or the ground.

Most regulations concerning silt fence specify a maximum perpendicular slope length for a given perpendicular gradient. United States Department of

9

Transportation (USDOT) design recommendations in Table 2.1 specify allowable slope lengths for a selection of upslope gradients perpendicular to a silt fence. Ideally, these slope lengths would be based on sediment load and flow rates. This would mean that the values given below should be adjusted for climatic conditions for a silt fence to ensure maximum effectiveness (Barfield and Hayes, 2000).

Table 2.1: Allowable slope lengths perpendicular to a silt fence (USDOT, 1995)

Slope (%)	18-inch (460 mm) Silt Fence	30-inch (760 mm) Silt Fence
< 2	250 ft (75 m)	500 ft (150 m)
5	100 ft (30 m)	250 ft (75 m)
10	50 ft (15 m)	150 ft (45 m)
20	25 ft (8 m)	70 ft (21 m)
25	20 ft (6 m)	55 ft (17 m)
30	15 ft (5 m)	45 ft (14 m)
35	15 ft (5 m)	40 ft (12 m)
40	15 ft (5 m)	35 ft (10 m)
45	10 ft (3 m)	30 ft (9 m)
50	10 ft (3 m)	25 ft (8 m)

2.1.3 Previous research. The majority of previous silt fence research focuses on the trapping efficiencies and hydraulic performance of a geotextile fabric barrier secured across the outlet of a laboratory flume. A standard design mixture of water and soil is released through the filter barrier, and the comparison of influent and effluent sediment concentrations yields a theoretical trapping efficiency (Wyant, 1980; Fisher and Jarrett, 1984; Crebbin, 1988; Kouwen, 1990; Jiang, 1997; and Britton, 2000).

This type of study originated with the Virginia Test Method (VTM-51) developed by the Virginia Highway and Transportation Research Council. Ongoing research has led to a better understanding of slurry flow rates and the

development of head-discharge relationships for both clear-water and sediment-laden flow through selected silt fence fabrics (Jiang, 1997 and Britton, 2000). Such studies provide important information on the hydrodynamics and sediment removal capabilities of silt fence under ideal conditions.

Jiang (1997) developed a head-discharge relationship for filter fabric by applying the Bernoulli equation to a single opening and then extending the principle to the entire cross-sectional area. An opening coefficient that varied with hydraulic head was introduced to simulate observed head-discharge conditions. A similar approach was used by Britton (2000) in analyzing head-discharge relationships for three different filter fabrics. A relationship for manufacturer specified opening size and effective opening area was developed, and the effective area was calculated using fabric discharge measurements. An indirect measure of opening size was applied by both Britton (2000) and Jiang (1997). Since parts of the orifice equation were determined by experiment, it is probable that unconsidered influences such as fabric stretching, experimental error, and apparatus characteristics were absorbed in empirical coefficients of head-discharge equations in both studies.

Silt fence performance studies conducted on test plots and on active construction sites can provide a better indication of actual field performance than in the lab environment. However, difficulties associated with monitoring storm water runoff events in the field can result in highly variable and non-representative data. In a study of silt fence installations on active highway construction sites, Barrett et al. (1995) observed median removal efficiencies of

0% for total suspended solids (TSS). The range in calculated efficiencies was −61% to 54% with a standard deviation of 26%.

A negative reduction signifies an observed increase in TSS downstream of the silt fence, which could result from minor sources of error such as disturbance of bottom sediments during sample collection. The sampling procedures allowed the determination of the removal efficiency of the silt fence alone and ignored removal attributed to sedimentation. Uncontrolled discharges caused by tears, overtopping, and undercutting failures were excluded from sampling, but results of the study still indicated poor performance of silt fence on active highway construction sites.

According to CERF (2001), performance issues related to compaction along the silt fence toe for traditional trenching and static slicing methods were compared in a field evaluation overseen and coordinated by the Environmental Technology Evaluation Center (EvTech), a program of the Civil Engineering Research Foundation (CERF). Thirty test segments were installed and tested on a gently sloping area using 30-ft-radius "smile" configurations without significant cross contour components in a predominately silty clay soil. Six 12-ft-radius smiles were evaluated, and ten straight 100-linear-feet segments were constructed to evaluate installation efficiency. An additional six runs were installed to compare installation methods on steep slopes, in rocky soils, and through wet spoils. Concentrated flow from a 2-inch diameter hose and a 5-hp pump created the 1,000-gallon runoff events, which were introduced within eight to ten minutes.

Three general types of trench-based installations were identified based on the likelihood of obtaining a fully backfilled and densely compacted trench. A comparison of storm water runoff retention was performed for the trench-based installation practices and the static slicing method. In general, the static slicing method was found to provide storm water runoff retention as good as or better than the best trench installations, and far superior retention when compared to common installation practices (CERF, 2001). The CERF (2001) study did not evaluate the performance of silt fence installed across contour lines; however performance trends from the study indicate that a greater level of compaction corresponds to better performance and fewer washouts.

Sprague (2002) conducted a field evaluation of silt fence performance based on observed modality of failure and compaction measurements with a handheld cone penetrometer on 56 active construction sites selected at random in 12 states. Results indicate that silt fence installed by the slicing method achieves higher compaction at the base of the fabric and is therefore less likely to washout than traditional trench-based installation practices. Static slicing was used on 26 sites, and the other 30 sites used trench-based installation practices. Forty percent of the trenched silt fences experienced undermining, and eight percent of the sliced silt fences experienced undermining. Slicing resulted in average relative soil strength of 83% based on the ratio of cone penetrometer testing results adjacent to the fence compared to the results of nearby undisturbed soil. Conversely, trenching resulted in 23% relative soil strength on

13

average. Average undisturbed soil strength for all sliced and trenched silt fence sites was approximately 300 psi (2070 kPa).

2.2 Challenges to the Effectiveness of Silt Fence

The irregularities and changing conditions of construction sites impact the performance of silt fence in a way that makes design criteria difficult to follow. The greatest challenges to the performance of silt fence are a result of inherent inadequacies, which compromise the function of silt fence as a flow retarding structure. The inadequacies are discussed along with their effects on impounding and diverting runoff in the following sections.

2.2.1 Observed inadequacies. Natural forces of water, wind, and sun all compromise the performance of silt fence even under the best design, installation, and maintenance conditions. However, deficiencies in performance of silt fence caused by improper design, installation, and maintenance give rise for concern. Observed inadequacies include: improper fabric splices, over-topping, torn fabric, under-runs due to inadequate toe-ins, and silt fence damaged or partially covered by the temporary placement of stockpiles of materials (Barrett et al., 1995). Additionally, CERF (2001) cites three improper installation practices associated with trench-based silt fence systems that lead to many of the problems associated with their use:

- Excavated soil from the trench is often inadequately backfilled or improperly compacted.
- Posts are installed in the trench prior to backfilling, preventing compaction equipment from contacting the full width of the trench.

- When the silt fence is not inserted to a uniform depth, shallow areas tend to washout more easily.

As previously cited, field evaluations by Barfield and Hayes (1992, 1999) in South Carolina and Kentucky indicate that installations on the contour as well as along a slope have problems with undercutting.

   2.2.2 **Impounding sediment-laden runoff.** In principle, a silt fence should distribute sediment-laden flow over an area of adequate storage capacity to pass the design flow without overtopping the fabric. However, inconsistencies abound when comparing the ideal silt fence to reality. First and foremost, construction sites are inherently irregular and frequently changing during early phases of earthwork. The capability for positioning a silt fence to collect sheet runoff considering spatial variability in topography is conceivable but impractical. Therefore, portions of silt fence must be used to direct flow toward areas of collection and sediment deposition (USEPA, 2002).

   Numerous studies have shown that sediment-laden flows cause clogging of fabric openings, dependent on the opening size and the size of sediment particles (Wyant, 1980; Fisher and Jarret, 1984; Barrett et al., 1995; Britton, 2000). In areas of quiescent flow and sediment trapping, sediment deposits along the base of the fabric and relatively clear water flows through the upper portion of unclogged fabric (Koerner, 1990). Thus, modeling studies need to be modified to account for the impacts of clogging on slurry flow rate.

   2.2.3 **Diverting sediment-laden runoff.** As previously mentioned, site limitations and topography make it impractical to install silt fence without diverting

overland flow along the base of the fabric. Sediment transport is a natural processes that silt fence is intended to control by reducing flow velocities and allowing sediment to deposit prior to leaving construction areas. However, sediment can potentially be detached from soil at the base of a silt fence when overland flow is diverted and becomes concentrated flow. The detachment of soil particles by rainfall in the area upslope of a silt fence is predominantly a result of raindrop impact and surface runoff in rills (Zhang, 2002). Detachment of soil particles at the base of a silt fence is mostly a result of concentrated flow erosion. The upslope area and toe trench both contribute sediment to the runoff when a silt fence diverts flow.

Sediment-laden flow that reaches a silt fence has a transport capacity depending primarily on soil type, flow rate, sediment load, and slope in the direction of flow movement. Transport capacity generally refers to the value to which sediment concentrations approach given that discharge and channel slope do not change. When sediment load exceeds sediment transport capacity, deposition occurs. Conversely, detachment of the backfilled toe trench is likely when transport capacity exceeds the sediment load transported from upslope areas. Barrett et al. (1995) suggests that, in the absence of sediment control measures such as silt fence, sediment-laden runoff flowing down a slope naturally deposits sediment at the toe of the slope as flow velocity decreases. In certain cases trapping or diverting the runoff could cause flow to concentrate and erode more soil than if flow was allowed to spread out with no control measures present. However, silt fence is often the most desirable way to curtail the flow of

sediment-laden runoff onto roadways and into storm drains. Its temporary nature promotes its use until more permanent stabilization practices can be implemented. The question remains: to what extent can silt fence impound or divert runoff and remain stable during a rainfall event of a particular design frequency?

2.3 *Modeling Silt Fence Performance*

Recent advances in modeling of sediment control structures have resulted in several new relationships. The WEPP watershed model is one example of a *continuous simulation* approach and includes computational procedures for a wide variety of sediment control structures (Lindley et al., 1998). Another example of a single storm-based model is SEDIMOT III (Barfield et al., 1996), which modifies the earlier SEDIMOT II model to include channel erosion routines and a wide variety of sediment control practices, including silt fence.

Considering these major advances, a drawback to the SEDIMOT III and WEPP silt fence routines is that they do not have a good technique for predicting the impact of cross contour components on the effectiveness of a silt fence. However, the basic processes that impact the performance of silt fence on a range of slopes can be simulated individually. Therefore, the basic hydrodynamic prediction techniques can plausibly be combined to develop modeling routines that simulate silt fence as a hydraulic structure encountering concentrated flow and scouring along its toe. The following sections describe components of a model that adequately simulates the processes influencing performance of a silt fence system.

2.3.1 Rill and Interrill erosion. Raindrop impact and surface runoff both play a part in the sediment delivered from a drainage area. Commonly accepted methods for predicting surface runoff from a design rainfall event are the Natural Resource Conservation Service (NRCS) Curve Number Method (NRCS, 1985) and the Rational Equation (WPCF, 1969). The Rational Method has many limitations and shortcomings (McPherson, 1969) and will not be used. The curve number method has been widely used due to its simplicity and available data. Curve number (CN) is estimated based on hydraulic soil group, land use, and antecedent soil moisture. An estimated runoff volume for a 10-year, 24-hour event can easily be determined and used for silt fence design. As a complement to the CN method, the NRCS-TR55 method (NRCS, 1986) is useful for estimating peak flow rate of a runoff event.

Sediment yield from upland erosion for a single storm can be estimated using the Modified Universal Soil Loss Equation (MUSLE) developed by Williams and Brendt (1972) using data from 778 storms on watersheds near Reisel, Texas and Hastings, Nebraska. The MUSLE equation for predicting single-storm sediment yield in tons is:

$$Y = 11.8(Q \times q_p)^{0.56}(K)(LS)(CP), \qquad (2.1)$$

where Y is single-storm sediment yield in metric tons, Q is runoff volume in m^3, q_p is peak flow in cms, and K, LS, and CP are USLE/RUSLE parameters for the drainage area. Using the runoff volume calculated from NRCS methods and the sediment yield predicted by MUSLE, an approximation of sediment concentration can be determined from a mass-based ratio of sediment to water (Haan, 1994).

2.3.2 Concentrated flow erosion. The focus of this thesis is on the impact of concentrated flow along the silt fence resulting from a cross contour configuration. Furthermore, it is postulated that the function of silt fence as an overland flow diversion or a flow retarding structure can be determined based on land slope along the fabric-soil interface. In the case of a flow diversion, spatially varied flow would result from runoff concentrating along a sloping segment of silt fence, causing concentrated flow erosion of the toe trench similar to the process of rill erosion. Thus it is important to review rill erosion relationships. Several different conceptual models for soil detachment in rills are available, including relationships involving flow discharge rate (Meyer and Wischmeier, 1969), hydraulic shear stress (Foster and Lane, 1983; Storm, 1991; and Nearing et al., 1989), and streampower (Yang, 1972; Nearing et al., 1997).

In modeling concentrated flow erosion, a relationship for detachment is needed. A basic detachment relationship is the shear excess concept used in the Foster and Lane (1983) model. The depth of flow along a silt fence creates a shear or tractive force on the trench backfill material, which is assumed to be more susceptible to detachment than the surrounding undisturbed soil. When estimating the erosion rate, the maximum shear force on the channel bottom is taken as:

$$\tau_{max} = 1.35 \gamma RS,$$
(2.2)

where τ_{max} is the maximum shear force on the channel bottom (Pa), γ is the specific weight of water (N/m^3), R is the hydraulic radius of the water in the channel (m), and S is the slope of the channel (m/m).

The potential rate of vertical erosion is then calculated by using soil erodibility with shear excess, or:

$$D_{rc} = K_r (\tau_{max} - \tau_c)^b,$$ (2.3)

where D_{rc} is the potential rate of vertical erosion (g/sec/m^2), K_r is the soil erodibility (s/m), τ_{max} is the maximum shear force on the channel bottom (Pa), τ_c is the critical tractive force of the bed material (Pa), and b is an empirical coefficient generally assumed to be 1.

Actual sediment detachment is modified to account for the ratio of sediment load to transport capacity as follows:

$$D_r = D_{rc}(1 - Q_s / T_c),$$ (2.4)

where D_r is actual vertical erosion at any point x along the rill (g/sec/m^2), D_{rc} is potential rate of vertical erosion at x (g/sec/m^2), Q_s is sediment load (g/sec), and T_c is transport capacity at x (g/sec). Transport capacity is discussed later.

Rate of downward movement in each rill segment is then estimated based on the ratio of actual vertical erosion to soil bulk density, or:

$$M_r = D_r / \rho_b,$$ (2.5)

where M_r is the rated of downward movement (m/sec), D_r is actual detachment (g/sec/m^2), and ρ_b is soil bulk density (g/m^3). Finally, the rate of downward movement can be used to predict the time required to erode a certain depth of a specified width of toe trench backfill material along a given length of silt fence.

An important aspect of erosion in rills and concentrated flow areas is the sediment transport capacity. Concentrated flow moving along a silt fence has a

sediment transport capacity that depends on soil type, flow rate, and slope. A sediment transport relationship based on unit stream power, defined as the time rate of potential energy expenditure per unit weight of water in an alluvial channel, is the dominant factor in determining total sediment concentration (Yang, 1972). The equation described by Yang (1972) relates transport capacity, or total sediment concentration, to unit stream power so that:

$$\log_{10} C_t = \alpha + \beta \log_{10}(VS - V_{cr}S), \qquad (2 \cdot 6)$$

where C_t is sediment concentration corresponding to sediment transport capacity (ppm), VS is unit stream power in (m/sec), $V_{cr}S$ is the critical unit stream power required for incipient motion, and α and β are parameters related to particle settling velocity and particle diameter.

Equation (2.6) was verified by 1,225 sets of laboratory data and 50 sets of field data. Most of these data showed a correlation of 0.98 or higher, and a standard error of estimate of 0.1 or less with the computed results from the equation. The two major drawbacks to Eq. (2.6) are lack of dimensional homogeneity, i.e., C_t is dimensionless, yet VS has the dimension of power per weight, and $V_{cr}S$ is not related to sediment and flow characteristics, but is determined by regression analysis. The Yang equation will not be used in this study, although Yang (1973) improves on the two drawbacks with a study of incipient motion.

One of the most commonly applied transport equations for small channels is the Yalin bedload equation. Yalin (1963) developed his bedload transport model for uniform, cohesionless grains over a movable bed. The model was

21

derived using dimensional analysis and the average grain motion for uniform

turbulent flow with a laminar sublayer that does not exceed the bed roughness.

Yalin (1963) first presented the model as several equations that were later

reduced by Alonso et al. (1981) to obtain an equation for sediment concentration

as:

$$C = 6.35 \times 10^5 \frac{SGdU_*}{vh} s \left[1 - \frac{1}{as} \ln(1 + as) \right],$$
(2.7)

where C is sediment concentration corresponding to sediment transport capacity

(ppm), SG is sediment specific gravity, d is average particle diameter (d_{50} in m),

U_* is bed shear velocity (m/s), v is average velocity (m/s), h is flow depth (m),

and a and s, the other two terms were defined by Yalin as:

$$a = 2.45 Y_{cr}^{1/2} SG^{-0.4} \quad \text{and} \quad s = \frac{Y}{Y_{cr}} - 1,$$
(2.8 and 2.9)

where Y_{cr} is the critical mobility factor, and Y is a mobility number defined by the

following equation:

$$Y = \frac{\rho_w U_*^2}{\gamma_s d}$$
(2.10)

To find the critical mobility factor, Shield's diagram is used to determine the value

for τ_c corresponding to a given roughness Reynold's number. This value for τ_c is

then used to determine a critical shear velocity, $U_{*c} = (\tau_c / \rho)^{1/2}$, which is then

used in Eq. (2.10) to determine Y_{cr}.

In summary, a combination of equations (2.2 and 2.3) for potential

detachment, equations (2.7 to 2.10) for transport capacity, and equations (2.4

and 2.5) for actual detachment can be used to model the depth of erosion at any point along a sloping segment of silt fence.

2.3.3 Sediment deposition and fabric flow. Fabric discharge and sediment deposition are the predominant physical processes affecting silt fence performance in areas of quiescent flow when silt fence functions as a flow-retarding barrier and not as a diversion. Numerous studies (Wyant, 1980; Crebbin, 1988; Kouwen, 1990; Jiang, 1997; and Britton, 2000) have evaluated fabric discharge characteristics, which are primarily a function of water depth, concentration of sediment, sediment size distribution, and fabric opening size. The amount of trapping in silt fence structures depends on the size of the structure, flow rates into the system, hydraulics of the flow control system, the size distribution of the sediment flowing into the structure, and the chemistry of the sediment-water system (Haan et al., 1994).

For steady-state flows, the trapping that occurs behind the silt fence can be shown to be directly proportional to the surface area and indirectly proportional to flow through the system (Haan et al., 1994). The ratio of the surface area to flow is known as the overflow rate, and trapping in such systems is predicted as a function of the ratio of overflow rate to particle settling velocity (Haan et al., 1994). Although flows in nature are inherently non-steady state and more complex than steady-state systems, studies have shown that the best predictor of trapping in such systems is still the ratio of settling velocity to overflow rate (Hayes and Barfield, 1995). In the case of non-steady state, the

23

overflow rate is best defined by the ratio of peak discharge from the system to the surface area of ponding (Hayes and Barfield, 1995).

The particle size distribution of eroded sediment is an important property affecting sediment transport and deposition (Haan et al., 1994). The particle size distribution for the upslope area and the toe trench backfill material soil matrix can be obtained via sieve and hydrometer analysis or from a particle size analyzer. An eroded particle size distribution can be approximated for the upslope sediment source area based on particle size estimation equations developed by Foster et al. (1985). The equations give an approximate soil fraction of five sediment particle classes: primary clay, primary, silt, small aggregate, large aggregate, and primary sand. It is important to distinguish between particle size distribution for the eroded and parent material since only eroded material is transported. However, the size distribution of parent material is assumed to approximate the eroded size distribution for non-cohesive materials.

Deposition of sediment takes place as flow velocities decrease and sediment load exceeds sediment transport capacity. Net deposition is calculated from the equation (Nearing et al., 1990):

$$D_f = (V_f/q)(T_c - G), \tag{2.11}$$

Where D_f is rate of deposition (kg/m^2/sec), V_f is effective fall velocity of the detached sediment (m/sec), q is runoff rate per unit width (m^2/sec), T_c is sediment transport capacity (kg/m/sec), and G is sediment load (kg/m/sec).

In areas of quiescent flow and sediment trapping, sediment deposits along the base of the fabric and relatively clear water flows through the upper portion of unclogged fabric (Koerner, 1990). The algorithms for fabric flow in SEDIMOT III are based on the assumption that clogging does not impact fabric discharge. However, numerous studies have shown that sediment-laden flows cause clogging of fabric openings, dependent on the opening size and the size of sediment particles (Wyant, 1980; Fisher and Jarret, 1984; Barrett et al., 1995; Britton, 2000).

Britton (2000) proposed a fabric discharge relationship that includes a modified orifice flow equation with a plugging coefficient related to fabric opening size. A bead mixture resembling the particle size distribution of a loam or silt loam soil was used to simulate sediment concentrations of 18000 to 43000 mg/L observed on an outdoor test plot of freshly tilled red sandy clay material. The results indicate satisfactory predictions of fabric flow for a limited selection of geotextile fabrics under clear-water and sediment-laden flow conditions.

2.4 Summary

Silt fence is one of the most cost effective and widely used measures for curtailing sediment-laden runoff on construction sites (DSC, 1998). Silt fences have been partially effective at removing larger particle sediment, primary aggregates, sands, and larger silts by capturing and slowly releasing overland flow (Horner, et al., 1990). Detention of sediment-laden water reduces flow velocities and transport capacity which leads to the deposition of sediment

upslope of the geotextile fabric. Although silt fence has been widely used, its performance in the field has not been well defined.

Proper design, installation, and maintenance practices play a critical role in the effectiveness of silt fence. However, design guidelines are often vague and impractical. Advanced installation methods for silt fence show potential for improving its performance. Static slicing is a proven silt fence insertion method with certain advantages to traditional trenching installation practices. Maintenance and disposal of silt fence poses a significant burden to contractors and should not be ignored in evaluating the performance and cost of silt fence.

Previous research on silt fence performance has shown high trapping efficiency in laboratory settings due in part to the use of sediment with larger diameters than the particles generally encountered in storm water runoff. Sediment removal by silt fences in the field has not been well documented due to difficulties in data collection. Information is needed on how the movement of water along a silt fence affects its performance and stability. Field studies could also be useful to characterize the performance of silt fence at various slopes and flow conditions.

Common problems encountered with silt fence include overtopping and undercutting due to inadequate design, installation, or maintenance practices. Silt fence functioning as a diversion of overland flow is prone to undercutting since runoff concentrates at the fabric-soil interface and exposes weak points in the toe trench. Three processes have been identified as the main components affecting silt fence performance:

1. Surface runoff and sediment yield from upslope areas,

2. Concentrated flow erosion at the base of a silt fence, and

3. Sediment deposition and factors related to fabric discharge.

The individual processes related to silt fence performance can be simulated and combined to model a silt fence system. Conceptualizing silt fence as a system with considerable flexibility to accommodate common site conditions would enhance modeling efforts and result in improved silt fence design capabilities. A process-based model that considers site-specific conditions would be useful for improving the effectiveness of silt fence and evaluating alternative design concepts. Examples of available relationships for developing such a model were reviewed in this section.

CHAPTER 3

EXPERIMENTAL EQUIPMENT

3.1 Adjustable Slope Test Flume

A series of fixed-bed and movable-bed flow tests were conducted indoors using a test flume located at the USDA-ARS Hydraulics Engineering Research Laboratory near Stillwater, Oklahoma. The apparatus shown in Figure 3.1 was constructed of metal, wood, and clear acrylic material and supported by a steel framework that allowed simple adjustment of bed slope from 0 to 8%.

Figure 3.1: Image of 0.5-ft (0.15-m) wide adjustable-slope trench with silt fence barrier
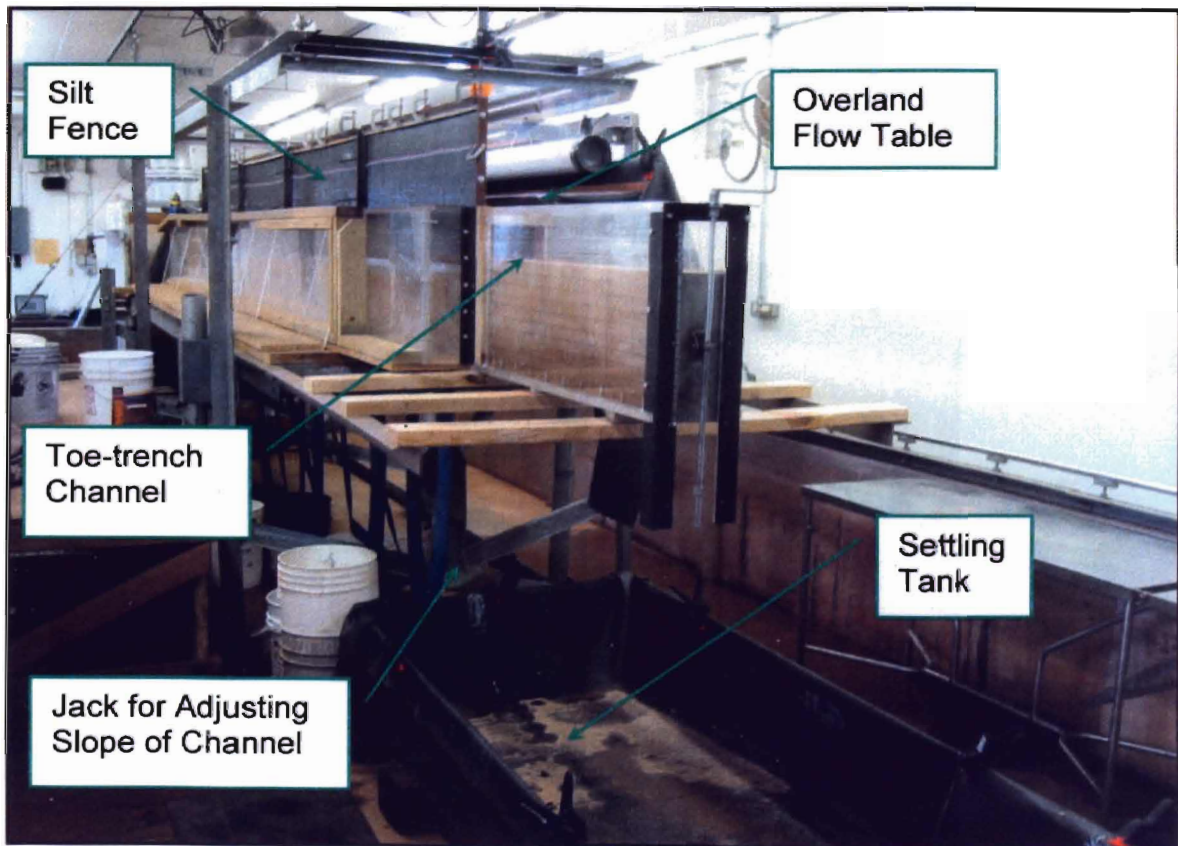
The central component of the test flume was a 0.5-ft (0.15-m) wide by 1.0-ft (0.30 m) deep channel formed from 20-gauge galvanized steel sheet material

to simulate a typical silt fence trench. One-inch steel "L" material was attached to the steel channel at a spacing of 4 ft (1.2 m) and served as silt fence posts to which the geotextile fabric was secured using three plastic cable ties through holes drilled in each post as shown in Figure 3.2 below.

Figure 3.2: Cross section of test flume configuration for fixed-bed study
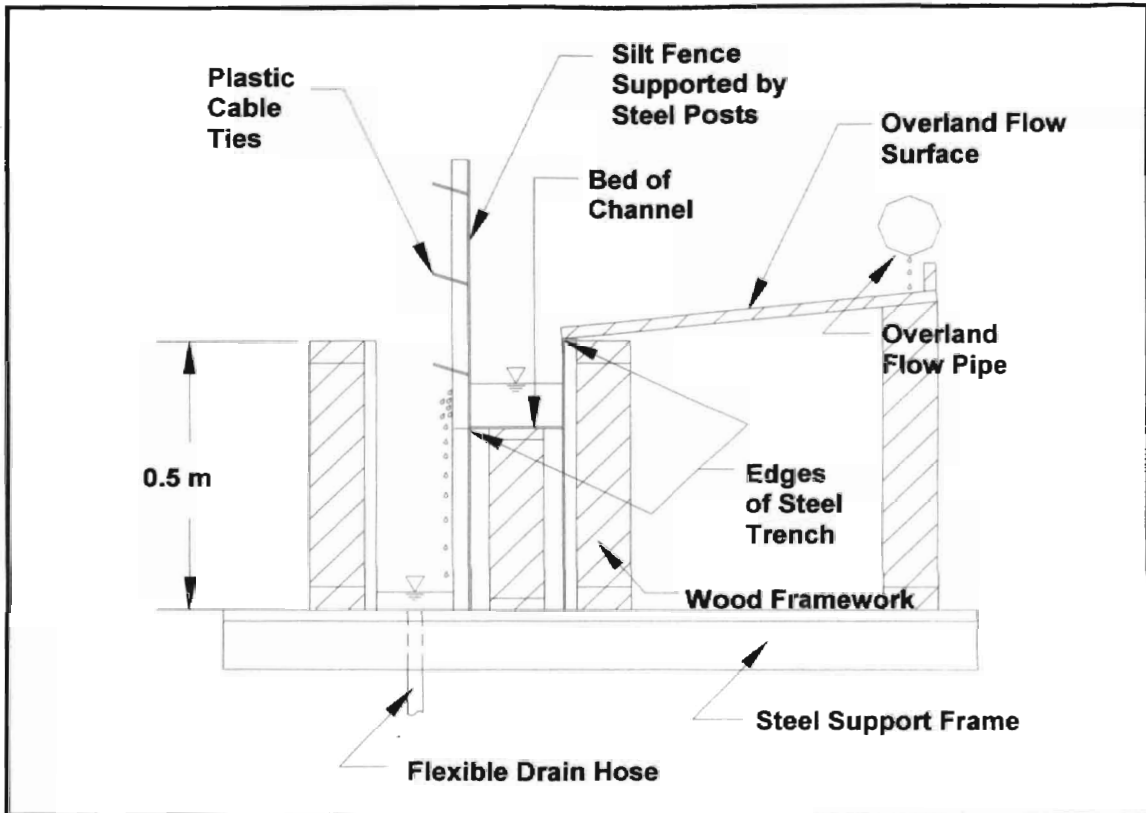
An overland flow surface (see Figure 3.2 above) sloping toward the silt fence at 10% was secured to the support channel directly above the steel trench. The clear-water flow supplied to the overland flow surface created a thin, evenly distributed sheet of water, such that the overland flow was clinging to the steel trench as it combined with the flow supplied by an upstream reservoir. An overland flow supply pipe consisting of a 10 ft (3.0 m) length of 4-in (10.2-cm) diameter PVC pipe with 40 evenly spaced 0.25-in (0.635-cm) orifices drilled

29

along its bottom was positioned above the overland flow surface. The inlet of the steel trench was attached to an upstream reservoir with rubber pond lining material (see Figure 3.3 below) that extended the length of the steel trench.

Figure 3.3: Rubber-lined connection of upstream reservoir to inlet of trench

Flow from a conceptualized upstream length of silt fence entered the test section of silt fence from the upstream reservoir as shown in Figure 3.3 above. The downstream end of the steel trench was connected to a 3 ft (0.9 m) clear acrylic channel with a matching cross section to allow for visual monitoring of flow depth, which was representative of flow conditions in the test section. Grid lines were marked at 0.1 ft (0.03 m) intervals, and an adjustable gate was used at the end of the test flume to control soil depth at the outlet during movable-bed

testing. Finally, a settling tank connected to an H-flume was positioned to collect and measure concentrated flow from the silt fence trench. Figure 3.4 shows the configuration of each component of the laboratory apparatus.

Figure 3.4: Profile view of experimental equipment configuration
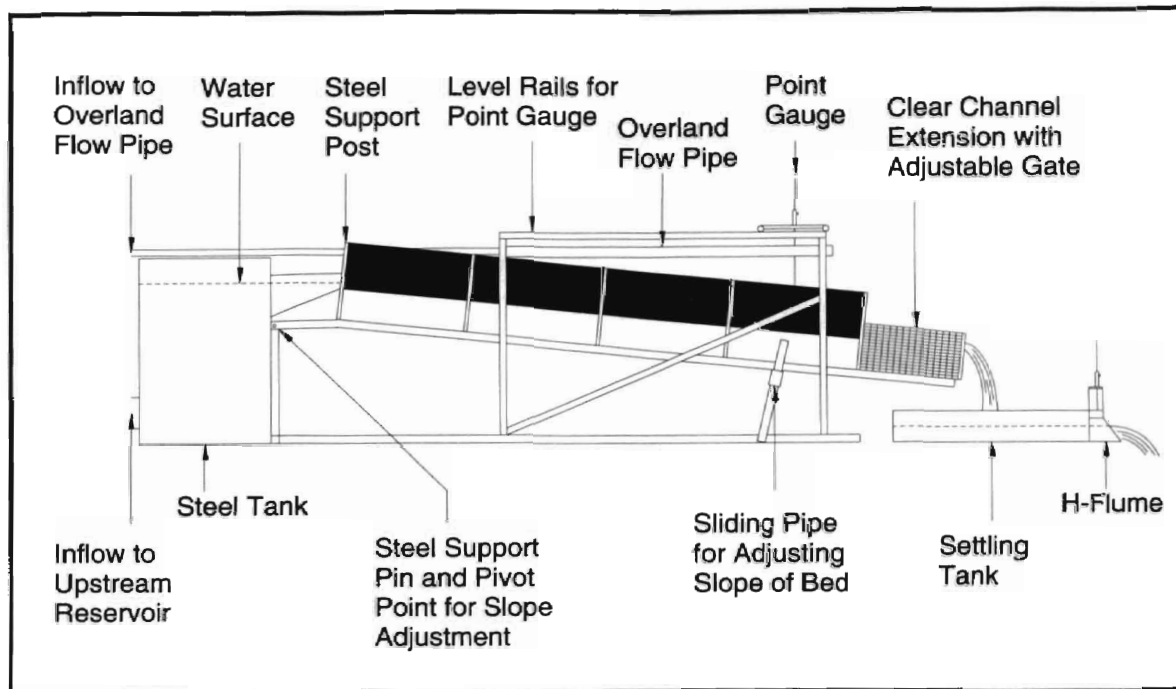
The geotextile fabric selected for the study was a woven polypropylene product labeled by Amoco (2002) as ProPex® 2130. The minimum average roll values for various physical properties are listed in Table 3.1.

Table 3.1: Vendor fabric specifications (Amoco, 2002)

Property	Test Method	Amoco 2130
Grab Tensile (lbs)	ASTM D 4632	124
Grab Elongation (%)	ASTM D 4632	15
Mullen Burst (psi)	ASTM D 3786	300
Puncture (lbs)	ASTM D 4833	65
Trapezoid Tear (lbs)	ASTM D 4533	65
UV Resistance (%/500hrs)	ASTM D 4355	80
AOS (US Sieve)	ASTM D 4751	30
Permittivity (sec^{-1})	ASTM D 4491	0.05
Flow Rate (gal/min/ft^2)	ASTM D 4491	10

31

3.2 *Measuring Devices*

Test flows were delivered to the model building by a gravity flow siphon from Lake Carl Blackwell and metered through a 2.500-inch (6.35-cm) diameter orifice with manometer tubes for measuring pressure drop across the orifice plate. The differential manometer with temperature calibration tables was used to regulate continuous flow with a precision of ±0.005 cfs (±0.00014 cms) entering the test flume through an upstream reservoir. A flexible 1.5-inch (3.81-cm) diameter hose was used to deliver flow to a pipe with orifices for simulating overland flow. The overland flow pipe was equipped with a pressure gauge, which was used to indicate and calibrate flow through the orifices for overland flow conditions. The pressure gauge had a range of 0 to 5 psi (0 to 34.5 kPa) and a precision of ±0.1 psi (±0.7 kPa).

A point gauge with a precision of ±0.001 ft (±0.0003 m) for measuring water surface and bed profiles was supported by a rolling carriage on a pair of level rails secured to a steel framework independent of the adjustable-slope test flume. A steel tape was used to designate horizontal stations to the nearest 0.01 ft (0.003 m) along the rails supporting the point gauge. A 10 ft (3.0 m) length of silt fence was designated as the test section for data collection, starting 6 ft (1.8 m) downstream of the inlet to the steel trench and ending at a point 1 ft (0.3 m) upstream of the union of the steel trench and the clear acrylic channel extension.

Flow through the fabric was divided into ten 1 ft (0.3 m) segments along the test section of silt fence. Flow from each segment was collected in a compartment, which drained through a flexible hose into a bucket. Fabric flow

was estimated for each segment by measuring the volume of water to the nearest 0.1 L collected over a set period of time, typically 15 minutes, representing approximately one fourth of the duration of each test. Flow that exited the test flume at the trench outlet was monitored with an H-flume by using a point gauge to record the depth of flow to the nearest 0.001 ft (0.0003 m). The accuracy of flow measurements corresponding to the point gauge depth readings was ±0.01 cfs (0.0003 cms).

Table 3.2: Measuring devices and corresponding accuracies

Description of Measurement	Measuring Device	Range of Measurements[1]	Precision[2]	Accuracy[3]
Upstream Flow	Manometer	55.0 inches	± 0.1 inch	± 0.02 %
Overland Flow	Dial Gauge	0.5 psi	± 0.1 psi	± 10.0 %
Fabric Flow	Beaker	3.0 L	± 0.1 L	± 3.3 %
Trench Flow	H-Flume (Pt. Ga.)	0.5 ft	± 0.001 ft	± 0.1 %
Vertical Distance	Point Gauge	3.0 ft	± 0.001 ft	± 0.03 %
Horizontal Distance	Steel Tape	9.0 ft	± 0.01 ft	± 0.1 %

1. Range of measurements was based on maximum recorded value (h) for each device.
2. Precision was based on minimum gradation (Δh) marked on each measurement device.
3. Accuracy was determined by linear error theory such that % accuracy = 100Δh / 2h for measurements of flow, and % accuracy = 100Δh / h for measurements of distance.

CHAPTER 4

METHODS AND PROCEDURES

4.1 Fixed-bed Study

A rigid boundary study was first used to evaluate the hydraulics of a silt fence and a sloping trench with steady-state flow conditions. The bed was constructed by placing fabric-covered steel panels on a wood support structure (see Figure 3.2). The clear water flow conditions selected for the fixed-bed study were based on a 10-year, 24-hour design storm of 5.2 in (132 mm) in Stillwater, Oklahoma. A high and a low flow were determined for respective drainage areas of 0.06 and 0.03 acres (243 and 121 m^2) using the NRCS-TR55 method to calculate peak discharges corresponding to the previously defined design storm.

Tests were conducted with and without simulated overland flow to evaluate the effects of spatially varied flow on the hydraulic performance of silt fence. The upstream reservoir, which simulated flow from an upstream length of silt fence, supplied the majority of flow to the test section. Overland flow was introduced to create spatially varied flow along the test section. Target slope and flow conditions for each test pair are summarized in Table 4.1.

Table 4.1: Target flows and silt fence slopes tested in the fixed-bed study

Test Pair	Slope (%)	Upstream Flow (cfs)	Overland Flow a, b (cfs)
1a, 1b	0.5	0.350	0, 0.07
2a, 2b	0.5	0.175	0, 0.07
3a, 3b	1	0.350	0, 0.07
4a, 4b	1	0.175	0, 0.07
5a, 5b	2	0.350	0, 0.07
6a, 6b	2	0.175	0, 0.07
7a, 7b	4	0.350	0, 0.07
8a, 8b	4	0.175	0, 0.07
9a, 9b	8	0.350	0, 0.07
10a, 10b	8	0.175	0, 0.07

Each test pair in Table 4.1 consisted of a specific slope and upstream flow setting studied with (a) and without (b) overland flow to isolate the effects of spatially varied flow. Three replicates of each test pair were completed using a random order of slopes for a total of 30 test pairs or 60 unique flow conditions. Each flow test typically required 60 minutes to collect all the required data. After allowing the flow to stabilize, measurements were taken to determine flow depth, fabric discharge, and trench discharge under steady-state conditions.

Point gauge readings were collected to determine flow depth along the centerline of the trench adjacent to a test section of silt fence. Flow through the fabric was collected and directed into ten 20 L plastic buckets over a known time to determine fabric discharge. Point gauge readings were monitored and compared to recordings from an electronic water level encoder in a stilling well connected to the H-flume, which gave an estimate of trench discharge based on the calibration curve in Appendix B relating H-flume discharge to depth of flow. A detailed summary of testing procedures is provided in Appendix A.

4.2 Movable-bed Study

Non-cohesive material (see Appendix C) was used to evaluate the performance of an erodible silt fence trench under a range of slope and flow conditions. The sand was placed in the steel trench at the base of the silt fence as described in Chapter 3. Wetting and draining the sand on a level slope provided uniform consolidation along the length of the simulated trench. The surface of the sand was then leveled using a special grading tool, and the bed slope was adjusted to the desired setting using a jack and support pins.

35

After collecting the initial bed profile with the point gauge, flow was released into the upstream reservoir. Flow conditions similar to those studied under fixed bed conditions were used with a selection of bed slopes from 0.0 to 4.5 percent. Final adjustments to the flow setting were made as the reservoir filled, thus allowing the desired flow to stabilize shortly after entering the trench. Manometer readings were checked during the brief time required to allow flow conditions to stabilize in the trench and catch basin connected to the H-flume.

Data collected during each test included total inflow, duration of flow, trench discharge, sediment concentration of the trench discharge, flow depth in the trench, initial and final bed profiles, and dry bulk density of bed material. Total inflow was controlled with a gate valve and metered through an orifice plate connected to a differential manometer. The height of the end gate at the trench outlet was adjusted based on visual monitoring of scour in the clear trench extension marked with 0.1 ft (0.03 m) grid lines.

Two to three sequences of measurements were recorded over the duration of each test. Sediment samples representative of total sediment load were collected at the outlet of the trench and later decanted and dried to determine the concentration of total solids (TS) for each test. Trench discharge was measured at the outlet of the catch basin with an H-flume, and flow depth was recorded by photographing the clear trench extension. Initial and final bed profiles were measured with a point gauge along the centerline of the trench.

CHAPTER 5

MODEL DEVELOPMENT

5.1 Description

According to Nearing et al. (1994), model development can be divided into two phases: creating a physical prototype and then numerically simulating the physical system. In this study, the process of model development began with the construction of a physical model of a silt fence system at the USDA ARS Hydraulics Laboratory near Stillwater, Oklahoma. Subsequently, a physically-based, steady-state mathematical erosion model was developed to predict the results of concentrated flow and sediment detachment in a simulated silt fence trench system. Methods and procedures related to the physical model were discussed in the preceding chapter, and the mathematical model will be described in this chapter.

A typical silt fence system can be conceptualized as a porous structure that collects runoff from a small drainage generating sediment-laden runoff. Under concentrated flow conditions, erosion of backfill material used to entrench the silt fence is similar to the process of rill erosion. The entrenched toe of fabric becomes susceptible to undercutting failure when silt fence converts overland flow runoff into concentrated flow along the backfilled soil in the trench. The processes resulting in rill formation and development have been studied and modeled in previous research (Meyer and Wischmeier, 1969; Foster and Meyer, 1972; Foster and Lane, 1983; Lu et al., 1987; Brown et al., 1989; Nearing et al.,

1989; Storm, 1991; and Wilson, 1993) and were considered in the development of the mathematical model.

A framework was developed for analyzing the performance of the idealized silt fence system installed at the laboratory. Performance of a silt fence was defined as the ability of an entrenched silt fence to withstand concentrated flow without the occurrence of undercutting under specific design conditions. The basic approach of the mathematical model is to segment overland flow along a section of silt fence and approximate spatially varied flow in order to estimate the detachment rate of the toe trench material at any point. Detachment potential of the flow, sediment load, transport capacity, and properties of the material used to backfill the trench are important parameters in predicting detachment rate.

5.2 Assumptions and Input Parameters

Certain assumptions were necessary to develop a mathematical model for predicting concentrated flow and detachment of soil in the idealized physical model. The assumptions related to open channel hydraulics were applied to both fixed-bed and movable-bed studies, while other assumptions were relevant only when modeling erosion for movable-bed conditions. The main assumption was that the test section of silt fence was of adequate length to develop uniform flow conditions without the addition of overland flow. When overland flow was added, segmenting the test section and assuming uniform flow in each segment gave an approximation of spatially varied flow conditions. In either case, the water moving along the test section of silt fence was assumed to achieve a predictable flow depth based on continuity of flow, trench slope, and channel roughness.

38

The small variation in measurements of flow depth from the average in each segment supported this assumption.

When predicting detachment rate for the movable-bed study, the sediment concentration of the flow entering the silt fence system was negligible and clear-water conditions were assumed. Soil density measurements were made and assumed to be representative of the bed material eroded during movable-bed tests. From the initial point of channel detachment, the entire width of the trench is assumed to erode downward at a constant rate. Although fluctuations in sediment transport rate are expected, the assumption of uniform scour is reasonable for the steady-state conditions tested in the movable-bed study.

For this study, a 10 ft (3 m) segment of silt fence was used as a test section with clear water inflow to the test section. This was assumed to represent the final segment of a silt fence subjected to flow entering from an upstream reach of fence and from an upslope drainage area. The following input parameters were required to adequately define the silt fence system:

- Slope (S), width (w), depth (d_t), and length (L) of the toe trench,

- Manning's n for the toe trench,

- Parameters in the head-discharge relationship for the silt fence (mA_{eff}),

- Simulated drainage area (A_{dr}) contributing overland flow to the silt fence,

- Precipitation volume (P) for a 10 year, 24 hour design storm,

- NRCS curve number (CN) for simulated drainage area,

- Representative particle diameter (d_{50}) for trench backfill, bulk density (ρ_b), critical shear stress (τ_c), and rill erodibility (K_r) for trench backfill material.

A critical distinction is made in the input parameters concerning the prevailing land slope and the slope of the toe trench. The prevailing land slope and slope length influences the rate of overland flow entering the fence, while the slope of the toe trench controls the movement of water along the silt fence and the resulting concentrated channel flow erosion.

5.4 Spatially Varied Flow

The test section of silt fence was simulated as a flow splitting structure with flow split between that moving down the trench and a small fraction of flow trickling through the porous fabric. Since overland flow was also introduced along the test section in part of the tests, the test section of silt fence was divided into three segments for modeling purposes to consider spatially varied flow.

The overland flow along the test section was divided evenly between the three segments, and spatially varied flow was approximated by accounting for flow entering and leaving each of the three segments. The overland flow entering a segment is represented by the following equation:

$$q\cdot = q_p / L , \qquad (5.1)$$

where $q\cdot$ is the overland flow (cms) to each segment, q_p is the simulated peak flow (cms), and L is the length of the silt fence test section (m).

The overland flow into each segment is then added to the flow from an upslope segment to calculate the total segmented flow as described by:

$$q_i = q\cdot + q_{i-1} - q_{fabric} , \qquad (5.2)$$

40

where q_i is the total flow (cms) in segment i, q. is the overland flow (cms) entering segment i, q_{i-1} is the flow (cms) entering from the segment upstream of segment i, and q_{fabric} is the flow through the silt fence in segment i.

Total flow in each segment is related to the geometry of the channel by the continuity equation and Manning's equation as follows:

$$q_i = (1 / n) \, S^{1/2} \, R^{2/3} \, A, \tag{5.3}$$

where n is Manning's roughness for the trench, S is slope of the energy gradient (m/m), R is hydraulic radius of the trench (m), and A is cross sectional area of flow (m^2). Hydraulic radius and cross sectional area of flow is related to flow depth by:

$$R = A / (2h + w) \qquad \text{and} \qquad A = wh,$$

where w is the width of the toe trench (m) and h is the depth of flow (m).

An objective function, $g(h)$, is minimized to find an iterative solution for depth of flow, h, in each segment such that:

$$g(h) = q_{\cdot} + q_{i-1} - q_i - q_{fabric} \tag{5.4}$$

The depth of flow in each segment is then used to estimate discharge through the silt fence fabric based on head-discharge relationships developed for certain fabrics by Britton (2000) or:

$$q_{fabric} = C' \, m \, A_{eff} (2gh)^{0.5}, \tag{5.5}$$

where q_{fabric} is the flow (cms), C' is an orifice coefficient (assumed to be a sharp-edged orifice with coefficient of 0.61), m is the number of openings contributing flow, A_{eff} is the effective orifice area for each opening (m^2), g is the gravitational constant (32.2 m/sec^2), and h is the hydraulic head acting on the fabric (m).

41

5.5 Sediment Transport

Soil detachment in concentrated flow channels results from excessive shear forces produced by concentrated flow, sidewall sloughing, and head cut advancement. Head cut advancement, due to its complexity and the lack of available physically based models, is neglected in the channel erosion model. For a constant flow rate, the channel shape in concentrated flow erosion has been shown to be rectangular with a constant width (Foster and Lane, 1983). In this model, the channel was assumed to be rectangular with a constant width of erosion equal to the width of the trench used in the lab study. Estimates of bed shear were based on the following equation for a laboratory flume:

$$\tau = \gamma h S , \tag{5.6}$$

where τ is shear stress (Pa), γ is specific weight of water (N/m^3), h is depth of flow (m), and S is slope (m/m).

The potential rate of vertical erosion is then calculated by using soil erodibility with shear excess, or:

$$D_c = K_r(\tau - \tau_c) , \tag{5.7}$$

where D_c is the potential rate of vertical erosion (kg/sec/m^2), K_r is the soil erodibility (s/m) (discussed in the following chapter), τ is the shear force on the channel bottom (Pa), and τ_c is the critical shear force of the bed material (Pa).

Actual sediment detachment was modified to account for the ratio of sediment load to transport capacity as follows:

$$D_r = D_c(1 - Q_s / T_c) , \tag{5.8}$$

42

where D_r is actual vertical erosion (kg/sec/m^2), D_c is potential rate of vertical erosion (g/sec/m^2), Q_s is sediment load (g/sec), and T_c is transport capacity (g/sec).

The concentrated flow moving along the toe trench has a sediment transport capacity that depends on the total sediment concentration. Since no sediment was transported to the toe trench by overland flow during the lab tests, a representative particle size (d_{50}) for the trench backfill material was used in sediment transport capacity calculations. Consistent with WEPP data analysis techniques, the sediment transport relationship used in the numerical model is that of Yalin (1963), represented in equations (2.7 to 2.10). A conversion of sediment concentration, C, to sediment load, T_c, is required for Eq. (5.8). The relationship used in the model is as follows:

$$q_s = \rho_w \, h \, C \,/\, 10^6 \tag{5.9}$$

$$\text{and} \quad T_c = 1000 \, q_s \, w, \tag{5.10}$$

where q_s is the sediment transport capacity per unit width of flow (kg/sec/m), ρ_w is density of water (kg/m3), h is depth of flow (m), C is the sediment concentration corresponding to sediment transport capacity (ppm), T_c is defined as the sediment transport rate corresponding to sediment transport capacity (g/sec), and w is the width of flow (m).

Rate of downward movement in each rill segment is then estimated based on the ratio of actual vertical erosion to soil bulk density, or:

$$M_r = D_r / \rho_b , \tag{5.11}$$

43

where M_r is the rate of downward movement (m/sec), D_r is actual detachment (kg/sec/m^2), and ρ_b is soil bulk density (kg/m^3). Finally, the rate of downward movement can be used to predict the time required to erode a certain depth of a specified width of toe trench backfill material along a given length of silt fence or:

$$t = d_t / M_r, \tag{5.12}$$

where t is the time required to erode the depth of backfill (sec), d_t is the depth of trench backfill material (m), and M_r is the rate of downward movement (m/sec).

Algorithms with related input parameters are listed in Table 5.1, and a flowchart in Figure 5.1 illustrates how the algorithms were linked in the spreadsheet-based model.

Table 5.1: Algorithms and input parameters used in the mathematical model

Reference in Text	Algorithm	Input Parameters
Eq. (5.1)	$q_* = q_p / L$	P, CN, L, and A_{dr}
Eq. (5.2)	$q_i = q_* + q_{i-1} - q_{fabric}$	See Eq. (5.5)
Eq. (5.3)	$q_i = (1/n)\, S^{1/2}\, R^{2/3}\, A$	n and S
Eq. (5.4)	$g(h) = q_* + q_{i-1} - q_i - q_{fabric}$	Iterations of h
Eq. (5.5)	$q_{fabric} = C'\, m\, A_{eff}\, (2gh)^{0.5}$	m and A_{eff}
Eq. (5.6)	$\tau = \gamma h\, S$	γ, S, and Eq. 5.4
Eq. (5.7)	$D_c = K_r(\tau - \tau_c)$	K_r and τ_c
Eq. (5.8)	$D_r = D_c(1 - Q_s / T_c)$	Eqs. (5.7 and 5.10)
Eq. (2.7)	$C = 6.35 \times 10^5\, \dfrac{SGdU_*}{vh}\, s\left[1 - \dfrac{1}{as}\ln(1+as)\right]$	v, h, SG, d, τ_c (from Shield's diagram)
Eqs. (2.8 and 2.9)	$a = 2.45 Y_{cr}^{1/2} SG^{-0.4}$ and $s = \dfrac{Y}{Y_{cr}} - 1$	SG and τ_c (from Shield's diagram)
Eq. (2.10)	$Y = \rho_w U_*^2 / \gamma_s d$	ρ_w, d, and γ_s
Eq. (5.9 and 5.10)	$q_s = \rho_w h\, C / 10^6$ and $T_c = 1000\, q_s\, w$	h and ρ_w
Eq. (5.11)	$M_r = D_r / \rho_b$	ρ_b
Eq. (5.12)	$t = d_t / M_r$	Eq. (5.11)

The flowchart in Figure 5.1 shows how the algorithms in Table 5.1 were combined to develop the framework of the mathematical model.

Figure 5.1: Flowchart representing the framework of the mathematical model

The symbols used in the diagram refer to parameters defined in the text.
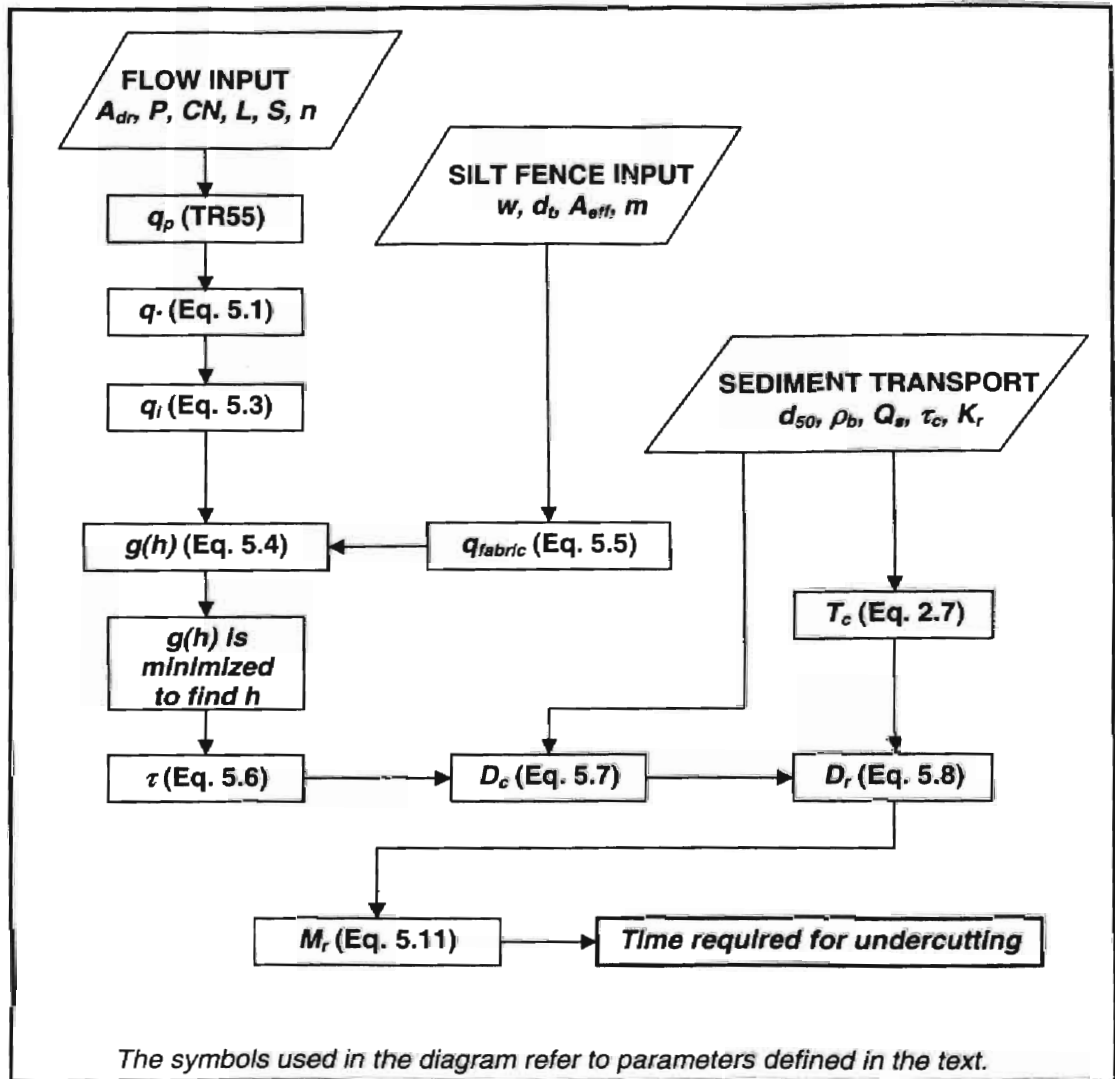
In summary, the depth of flow in each segment is estimated based on a continuity equation relating overland flow, toe trench open channel hydraulics, and hydraulics of the fabric. Then soil detachment is determined using concentrated flow erosion equations based on shear excess and transport capacity. Finally, the time, t, required to erode a specified depth is computed.

CHAPTER 6

RESULTS AND DISCUSSION

6.1 Introduction

A series of laboratory tests were conducted to provide experimental data for evaluating model predictions of the hydraulic and sediment transport processes. A fixed-bed apparatus (see section 4.1) was first used to collect hydraulic data and to analyze the performance of silt fence with a sloping trench under steady-state flow conditions. All test pairs were completed using the same silt fence over a period of five months beginning in August 2002. A test pair was defined as a specific slope and upstream flow setting studied with and without overland flow to isolate the effects of spatially varied flow. Three replicates of each test pair were completed using a random order of slopes for a total of 30 test pairs or 60 unique flow conditions. Half of the tests were conducted with continuous upstream flow only, and overland flow was added for the other half of the tests to isolate the effects of flow addition along the test section.

Movable-bed tests were conducted with the same piece of silt fence used in the fixed-bed study to collect concentrated flow erosion data and to evaluate the performance of a silt fence trench backfilled with highly erodible non-cohesive soil for a range of slope and flow conditions (see section 4.2). Testing of movable-bed conditions required a total duration of three months ending in March 2003. Nine different flow and slope settings were studied without overland flow. The results of fixed-bed and movable-bed studies are presented, discussed, and compared to model predictions in the following sections.

6.2 Results of Fixed-Bed Study

The silt fence acted as a porous structure with a small fraction of flow discharging through the fabric as water moved downslope along the silt fence trench. Average measurements and calculations for each slope and flow setting used in the fixed-bed study are summarized in Table 6.1. Each row of data in Table 6.1 represents the average value of three repetitions at the specified slope and flow settings. Data for all tests are provided in Appendix C.

Table 6.1: Data analysis for fixed-bed study (each row is average of three repetitions)

Slope, S (m/m)	Flow Rate, Q (cms) Upstream	Flow Rate, Q (cms) Overland	Fabric Flow (cms)	Ave. Depth, h (m)	Ave. Vel.[1] (m/sec)	Ave. Shear[2] (Pa)	n[3]	F[4]
0.005	0.005	0.000	1.4E-05	0.044	0.753	2.18	0.009	1.2
0.005	0.010	0.000	5.1E-05	0.072	0.946	3.54	0.008	1.2
0.01	0.005	0.000	1.2E-05	0.033	0.975	3.27	0.008	1.7
0.01	0.010	0.000	2.2E-05	0.054	1.211	5.27	0.008	1.7
0.02	0.005	0.000	6.2E-06	0.029	1.141	5.59	0.009	2.2
0.02	0.010	0.000	2.3E-05	0.046	1.416	9.01	0.009	2.1
0.04	0.005	0.000	8.1E-06	0.023	1.390	9.17	0.010	2.9
0.04	0.010	0.000	1.8E-05	0.039	1.673	15.25	0.010	2.7
0.08	0.005	0.000	6.2E-06	0.018	1.874	13.88	0.009	4.6
0.08	0.010	0.000	1.6E-05	0.032	2.034	25.10	0.011	3.6
0.005	0.005	0.002	4.5E-05	0.278	0.385	4.15	0.017	0.4
0.005	0.010	0.002	1.0E-04	0.392	0.546	5.85	0.012	0.5
0.01	0.005	0.002	4.2E-05	0.202	0.790	6.03	0.016	1.1
0.01	0.010	0.002	6.9E-05	0.300	0.716	8.96	0.015	0.8
0.02	0.005	0.002	1.9E-05	0.151	0.710	9.00	0.014	1.1
0.02	0.010	0.002	3.3E-05	0.201	1.061	12.02	0.011	1.4
0.04	0.005	0.002	1.5E-05	0.115	0.933	13.69	0.016	1.6
0.04	0.010	0.002	4.0E-05	0.167	1.284	19.94	0.011	1.8
0.08	0.005	0.002	9.0E-06	0.085	1.250	20.42	0.013	2.5
0.08	0.010	0.002	1.9E-05	0.125	1.715	29.80	0.009	2.8

1. Ave. Vel., $V = Q / A$, where $A = hw$ and width of flow in trench, $w = 0.15$ m
2. Ave. Shear, $\tau = \gamma h S$, where γ for water at 25 °C is 9777 N/m^3
3. Mannig's $n = S^{1/2} R^{2/3} / V$ (Eq. (6.1) was used for tests with overland flow)
4. Froude number, $F = V / (gh)^{1/2}$

6.2.1 Manning's 'n'. After estimating average flow velocities using the continuity equation described in the first annotation of Table 6.1, values of

Manning's 'n' (roughness) were calculated for uniform flow conditions by solving Manning's equation for n. Flow velocity increased with slope as expected, and calculated values of roughness ranged from 0.007 to 0.012 for all fixed bed tests with only upstream flow. The average value used in calculating predicted flow depths was 0.009 for tests with no overland flow.

The Manning's equation for uniform flow did not apply to the test conditions where overland flow was added, since the addition of overland flow caused spatially varied flow conditions. Therefore, the dynamic equation for spatially varied flow with increasing discharge was solved for Manning's n to determine an average channel roughness value. Chow (1959) presents the following equation for spatially varied flow based on momentum change along a representative section of channel:

$$\frac{dy}{dx} = \frac{S_0 - S_f - 2Qq_\ast/gA^2}{1 - Q^2/gA^2D}, \tag{6.1}$$

where dy is the change in depth for a unit length (dx) of channel, S_0 is the slope of the channel bed, S_f is the friction slope represented by the Manning's formula as $S_f = Q^2n^2 / 2.22A^2R^{4/3}$, Q is the discharge at the upstream end of the channel section, $q_\ast$ is the added discharge per unit length of channel ($q_\ast = dQ/dx$), g is the gravitational constant, A is the cross sectional area, and D is the hydraulic depth.

Measured values were substituted into Eq. (6.1) for all parameters except n, which was determined by iteration in the relationship for S_f such that dy/dx in Eq. (6.1) matched observed dy/dx values. Average Manning's n values were slightly higher for the test conditions with addition of overland flow and ranged from 0.009 to 0.017 with an average value of 0.013 used for modeling purposes.

6.2.2 Depth of flow. Average values of Manning's roughness were used

to predict flow depths in the numerical model when simulating the hydraulic

performance of a silt fence with a non-erodible trench. A comparison of

observed and predicted flow depth for conditions of upstream flow without

overland flow is presented in Figure 6.1 below. The relationship of observed and

predicted depths of flow in Figure 6.1 has a 0.0001 m^2 sum of squared error.

Figure 6.1: Comparison of predicted and observed depths of flow for upstream flow only
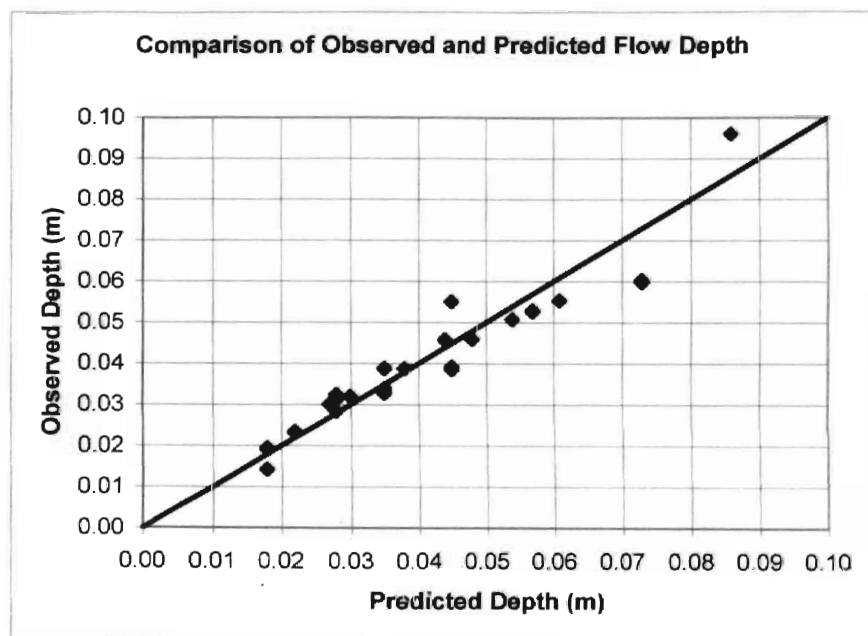
The comparison in Figure 6.2 shows the relationship of observed and

predicted depths of flow with the addition of overland flow. The predicted depths

were computed based on measured flow rates and cross sectional area with

average Manning's n based on the spatially varied flow relationship described by

Eq. (6.1). The sum of squared error was 0.01 m^2 for the data in Figure 6.2. More

scatter was apparent in the overland flow comparison (see Figure 6.2) due to

greater fluctuation in measured depths of flow.

Figure 6.2: Comparison of predicted and observed depths of flow for overland flow tests

Comparison of Observed and Predicted Flow Depth
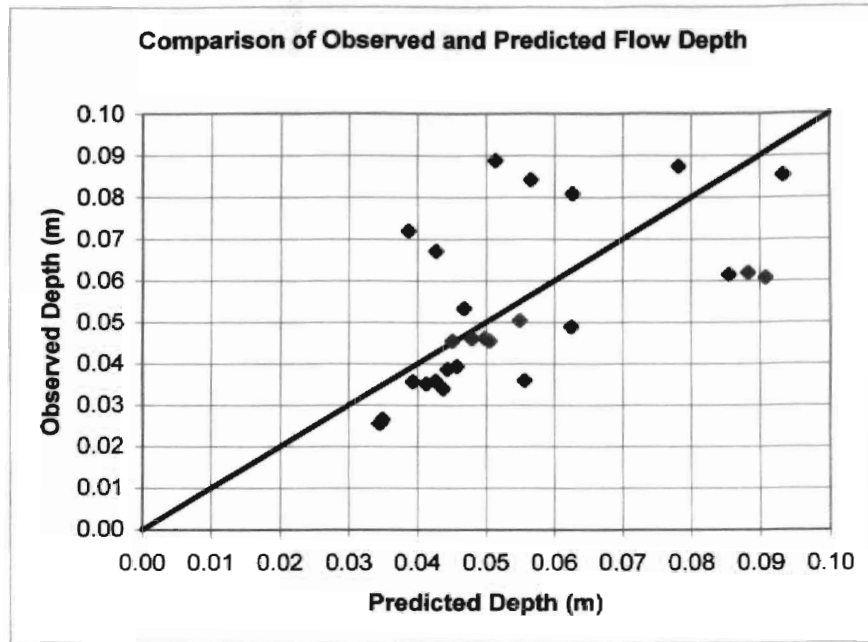
6.2.3 Bed shear. Average bed shear was estimated by Eq. (5.6) for all

tests based on slope settings and measurements of flow depth. Figure 6.3

shows the range of bed shear estimates for the slope and flow conditions tested.

Figure 6.3: Range of bed shear conditions tested at each bed slope in fixed-bed study

Bed Shear as a Function of Slope
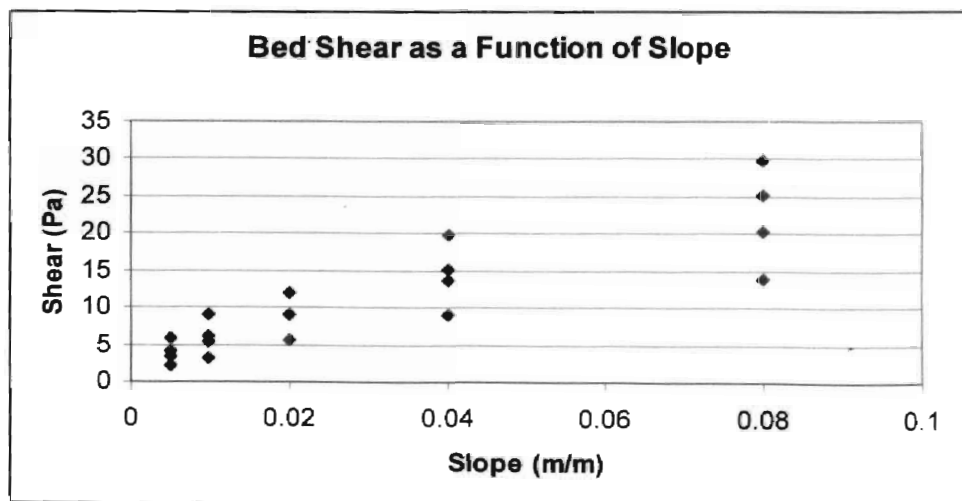
6.2.4 Fabric flow. Fabric discharge was measured for each 1 ft (0.3 m)

segment of silt fence in the 10 ft (3 m) test section. The total fabric flow for the

test section was calculated and compared to predicted flow based on a modified

orifice equation developed by Britton (2000) for the fabric used in this study. The

observed relationship between depth of flow in the fabric trench and fabric

discharge through a 3.0 m segment of silt fence is represent below in Figure 6.4,

which includes all data for the sloping-trench, fixed-bed study.

Figure 6.4: Discharge through silt fence for all fixed-bed test conditions

Fabric Discharge as a Function of Depth of Flow

- ◆ Series1 $Q = 0.0031H^{1.38}$ ($R^2 = 0.7987$)
- ■ Series2 $Q = 0.0074H^{2.23}$ ($R^2 = 0.9337$)
- ▲ Series3 $Q = 0.0029H^{1.91}$ ($R^2 = 0.9237$)
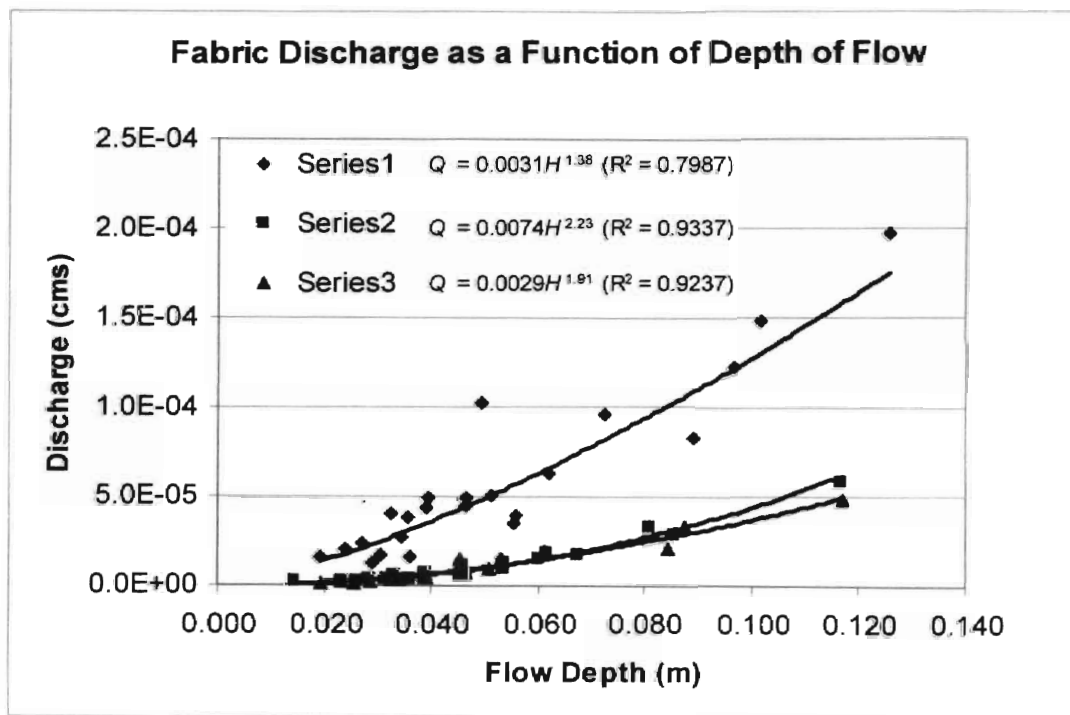
The three data series in Figure 6.4 represent three repetitions of the same

test conditions. Non-linear regression was used to fit a power function through

each of the data sets, and the first set of data was consistently higher than the

other two sets of data. Considering that test conditions were carefully controlled

in a laboratory, the variation in head-discharge relationships between Series 1

and the other two data sets was not expected. Tl

used for all tests, and each data set required 20 l

temperature could explain part of the variation sir

collected prior to the other two data sets. Anothe

of the silt fence could have been altered after the

have been a result of a physical, chemical, or bio

Physical clogging of the fabric openings w

the water supply is a plausible explanation; howe

also merits consideration. Inadvertent stretching

of testing would result in a change in the head-di

the fabric could increase the size of the openings

area of discharge; however a converse effect is ;

more detail in the following sections.

Observed head-discharge relationships fc

settings were compared to expected values of fa

depth of flow as described in Table 6.2 below.

Table 6.2: Data analysis for fabric dis

| Depth of Flow (m) | Fabric Flow (cms x 10^4) Determin< | |
	Sloping Trench Data	Level Trench Data
0.00	0.0	0.0
0.03	0.2	0.8
0.06	0.6	2.5
0.09	1.1	4.9

1. Predicted values were determined from equatior

2. ASTM 4491 method was used by Amoco (2002)
value of 10 gpm per ft^2, which was used to calcula<
silt fence with the indicated depth of flow.

More unexpected discrepancies emerged when the observed data were compared to the predicted head-discharge relationships as shown in Figure 6.5.

Figure 6.5: Comparison of measured and predicted fabric flow relationships
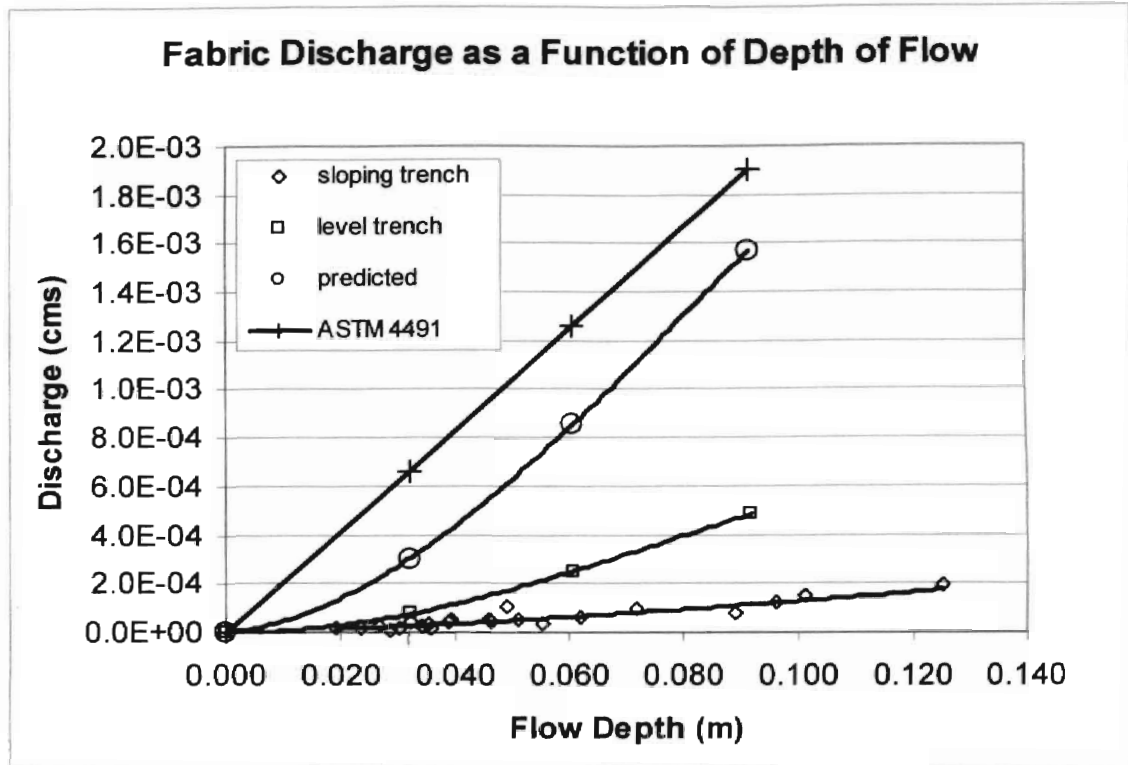
Britton (2000) results (labeled as predicted in Figure 6.5) for the filter fabric used in this study were based on data collected using a new piece of silt fence for each flow test, and the fabric used for this entire study demonstrated a reduction in discharge by a factor of three after the first data set was collected (see Figure 6.4). The observed head-discharge relationship for the level trench (see Figure 6.5) was expected to follow the predicted relationship developed by Britton (2000) for a filter fabric identical to one used in this study. However, fabric discharge results from the level trench tests indicate that, similar to the reduction in discharge illustrated in Figure 6.4, observed flow rates for the level

trench were lower than the predicted flows by factors of three or more as shown in Figure 6.5. It should be noted that the level trench tests were performed at the end of the fixed-bed study, thus the fabric at that time had been subjected to nearly 60 hours of clear-water flow taken from a lake through metal pipes.

Prediction equations developed by Britton (2000) are dependent on an opening area parameter calculated from experimental data for head and discharge. Since the effective area of fabric openings is determined by experiment, the area calculations absorb unconsidered influences like stretching, sagging, or micro plugging of the filter fabric. A likely explanation of the factor of three plus variation turning up in two independent comparisons is that hydraulic characteristics of a silt fence are significantly altered with time even when subjected to flows with scant sediment loads. These results indicate that a new piece of silt fence can discharge three times as much flow as a silt fence that has experienced flow.

Another possible explanation for the lower than expected fabric discharge is the movement of water parallel to the silt fence. A head loss due to the velocity of flow along the fabric would effectively reduce the discharge through the fabric when compared to fabric discharge resulting from hydrostatic head along a section of silt fence. In the case of hydrostatic conditions, the momentum of flow is all directed through the silt fence. Whereas, in the case of flow moving parallel to the fabric, a change in momentum is required for the flow to pass through the silt fence, thus resulting in an effective loss in head.

A simplistic approach to correlating the observed and predicted head-discharge relationship is to develop a correction factor based on observed fabric flow for the level slope setting. The correction factor could then be included in the modified orifice equation used to predict fabric discharge as follows:

$$C_c = q_{f, \text{ measured}} / q_{f, \text{ predicted}},$$

where C_c is the correction factor for relating observed level slope flow to predicted, $q_{f, \text{ measured}}$ is the power function relating measured flow to depth of flow, and $q_{f, \text{ predicted}}$ is the relationship developed by Britton (2000). Since both relationships include a term close to $H^{1.5}$, the correction factor could be assumed to be constant for the case of a level trench. It was determined that the correction factor is approximately 3.5 using all measured head-discharge data and fabric-specific parameters developed by Britton (2000). Such a correction factor could potentially be used to examine the effects of concentrated channel flow velocity on reduction in head acting on the fabric. However, the usefulness of such a correction factor should be limited to conditions similar to those tested in the lab study. Further study is needed to develop additional relationships.

6.2.5 Discussion of results. In summary, the flow conditions tested in a non-erodible silt fence trench with a rectangular cross section were predictable for the selected range of trench slopes. Manning's roughness estimates resulted in a moderate range of values with no evidence of a trend related to slope, flow depth, or flow velocity. The average roughness value was used in Manning's equation along with the continuity equation to compute depth of flow assuming uniform flow conditions.

Predicted flow depths correlated well with observed depths of flow, but fabric discharge measurements did not follow the expected head-discharge relationship developed by Britton (2000). One possible technique for correcting the flow prediction equation is to add an energy loss term associated with flow velocity along a segment of filter fabric. Another approach would be to reconsider the method of approximating effective opening area and introduce coefficients to the modified orifice equation that account for influences of fabric tightness on the head-discharge relationship.

Fabric tightness logically contributes to the head discharge relationship of filter fabric, but determining the effects of fabric tightness was beyond the scope of this study. The woven configuration of fabric filaments is inherently flexible and allows the force of water to stretch and pass through openings when the filaments are not secured to posts in a taut position. Consequently, a tightly stretched section of silt fence would have a smaller effective opening area when compared to a less tightly stretched section of the same fabric. Discharge is most likely reduced when silt fence is secured in a taut configuration as compared to discharge for the same depth of water through sagging fabric.

6.3 Results of Movable-Bed Study

The purpose of the movable-bed study was to determine the effects of trench slope on the performance and stability of a silt fence. An additional use of the data collected for this portion of the laboratory study was to validate the modeling routines developed for concentrated flow erosion along a silt fence on a range of slopes similar to those tested in the experiments. Results for eight

different trench erosion test conditions were analyzed, and a summary of the

data analysis is provided in Table 6.3 below. More complete data sets are given

in Appendix E.

Table 6.3: Results and data analysis for movable-bed tests

Test (No.)	Slope (%)	Q (cfs)	h (ft)	V (fps)	Q_s (g/sec)	τ (Pa)	T_c (g/sec)
1	1.0	0.17	0.18	1.89	5.0	5.4	83
2	2.4	0.15	0.11	2.78	77.3	7.9	238
3	0.8	0.17	0.19	1.76	3.5	4.5	56
4	4.5	0.16	0.08	4.10	215.7	10.8	483
5	0.4	0.17	0.20	1.71	3.3	2.4	13
6	1.1	0.34	0.20	3.41	4.6	6.6	112
7	2.4	0.34	0.18	3.82	95.6	12.9	418
8	4.3	0.33	0.15	4.33	351.6	19.3	945

Visual monitoring of bed forms during each test gave some indication of

flow conditions. The bed forms consisted of small ripples with little effect on the

movement of water for tests 1, 3, 5, and 6. Flow conditions were less stable, and

bed forms began to affect the water surface during tests with slopes greater than

one percent. Formation of dunes and anti-dunes moving upstream was noted for

tests 2, 4, 7, and 8, with rapid detachment of bed material during tests 4 and 8.

The clear channel extension provided a one-meter length of flow visualization,

which provided a representative profile of the entire channel. Depth of flow, h,

was determined by analyzing grid lines present in digital images recorded of the

clear channel extension during each test. Sample images used in the analysis

are provided in Appendix F.

Velocities in Table 6.3 were computed based on the continuity equation

using the ratio of direct flow measurements to cross-sectional areas determined

from measured depths of flow. Measured sediment concentrations were

multiplied by flow rate to obtain the rate of sediment discharge, Q_s. Values of bed shear, τ, were computed using Eq. (5.6). Transport capacity, T_c, for each test condition was then estimated using Eq. (5.10). The results in Table 6.3 follow expected trends when comparing changes in slope and flow conditions to changes in sediment transport.

6.3.1 Erodibility and critical shear. A method of determining rill erodibility and critical shear was needed to develop the required input parameters for the model described in section 5.5. Data analysis techniques used in WEPP were selected to arrive at the required input parameters. The transport capacity, channel width, and observed rate of sediment leaving the trench were first used to calculate the detachment capacity for each test condition according to the relationship developed by Elliott et al. (1989), which assumes constant shear along a rill such that:

$$ D_r = \frac{-T_c}{w_r L} \ln\left[\left(1 - \frac{Q_s}{T_c}\right)\left(\frac{D_c'}{D_r' + E}\right)\right], \tag{6.2} $$

where L is rill length (m), w_r is rill width (m), T_c is transport capacity (g/sec), and Q_s is sediment delivery rate (g/sec) measured at the downstream end of the rill. D_c' and E are factors related to interrill erosion, and E is zero in the case of clear water flow in a rill. Therefore, the final term in the logarithm of Eq. (6.2) drops out of the relationship for conditions tested in this study.

As discussed in a previous chapter, detachment capacity, D_c, is the capacity of clear water to remove bed material, and actual detachment rate, D_r, accounts for the effective reduction in detachment capacity due to the ratio of

sediment load to transport capacity. Detachment capacity, D_c, was then substituted into Eq. (5.8) to estimate actual detachment rates, D_r. Values for rill erodibility, K_r, and critical shear, τ_c, were then calculated by linear regression from detachment rate as a function of hydraulic bed shear as shown in Figure 6.4 below.

Figure 6.4: Linear approximation of detachment rate as a function of bed shear
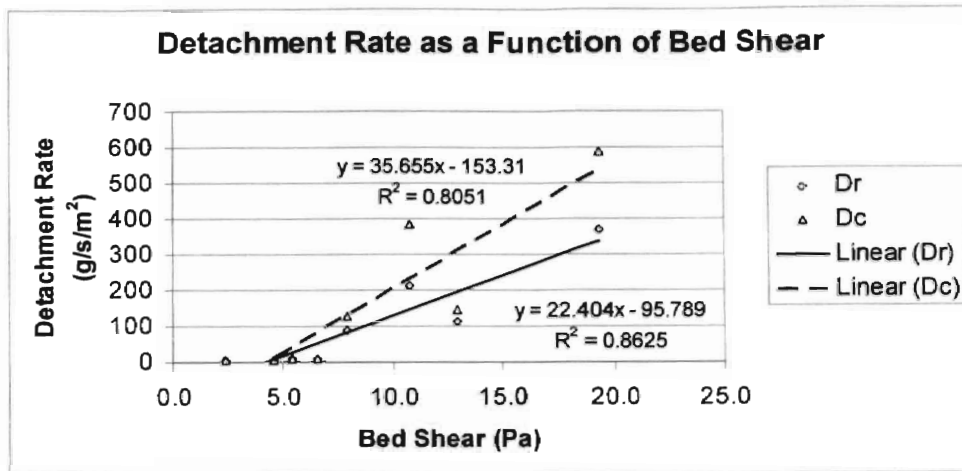
Rill erodibility (slope/1000) was estimated at 0.036 s/m, and critical shear for the erodible bed material was approximately 4.3 Pa (x-intercept) based on the linear relationship of detachment capacity to bed shear as described by Eq. (5.8) and illustrated in Figure 6.4. A summary of detachment rates used in the determination of rill erodibility and critical shear is presented below in Table 6.4.

Table 6.4: Detachment rates used to estimate soil erodibility parameters

Test	Slope	h	τ	D_r	D_c
(No.)	(%)	(ft)	(Pa)	(g/s/m^2)	(g/s/m^2)
1	1.0	0.18	5.4	7	7
2	2.4	0.11	7.9	84	125
3	0.8	0.19	4.5	5	5
4	4.5	0.08	10.8	211	381
5	0.4	0.20	2.4	4	5
6	1.1	0.20	6.6	6	6
7	2.4	0.18	12.9	112	145
8	4.3	0.15	19.3	368	586

The estimated values of K_r and τ_c for the soil used in the laboratory study were used to predict detachment rates. A comparison of observed and predicted values of detachment rate is shown in Figure 6.5 below.

Figure 6.5: Comparison of detachment rate based on measured sediment loads to predicted detachment rate based on average erosion parameters (K_r and τ_c).
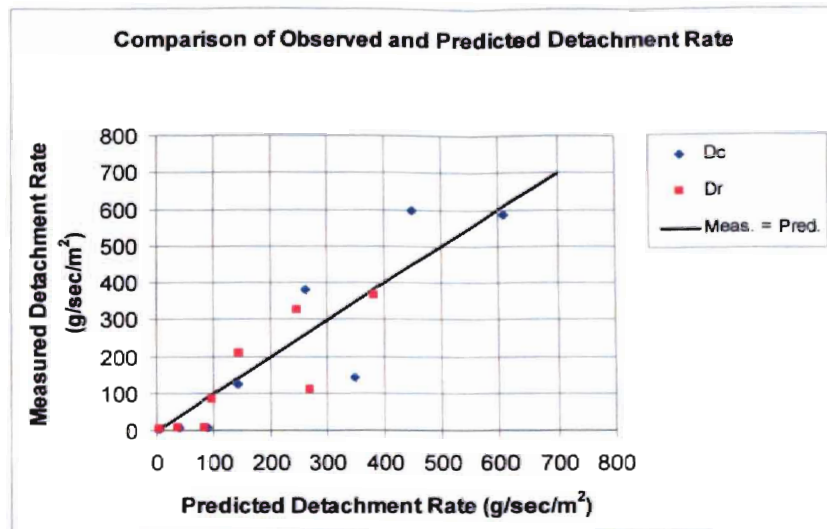
The values compared in Figure 6.5 indicate that the use of average soil erodibility parameters, K_r and τ_c, resulted in predicted detachment rates reasonably close to the measured detachment rates for both detachment capacity, D_c, based on the shear excess relationship and for actual detachment, D_r, or the detachment that accounts for the influence of transport capacity. Standard error of estimation was determined to be 102 g/sec/m^2 for D_c and 77 g/sec/m^2 for estimates of D_r.

6.3.2 Evaluation of model predictions. The estimated values of K_r and τ_c for the soil used in the laboratory study were then used to predict net detachment for an independent test, which was excluded from the determination of experimental values of K_r and τ_c. During the independent test, flow continued

until the average scour depth was greater than the depth required to cause undercutting. The modeling framework described in Chapter 5 was applied to arrive at a predicted depth of flow, sediment transport rate, and net scour over a time equal to the duration of the independent test. A summary of results for the independent test and model predictions is provided below in Table 6.5.

Table 6.5: Model predictions and comparisons for an independent test

Equation No.	Parameter	Observed Value	Predicted Value	Percent Error
5.4	Flow Depth, h	0.037 m	0.035 m	5%
5.5	Fabric Flow, q	NA	NA	NA
5.6	Bed Shear, τ	15.4	14.8	4%
6.1(obs.) 5.7(pred.)	D_c	600 g/sec/m^2	378 g/sec/m^2	37%
5.8	D_r	326 g/sec/m^2	206 g/sec/m^2	37%
Basis of Comparison	Scour Depth, d_t	0.23 m	0.23 m	NA
5.12	Req. Time, t	1800 sec	1667 sec	7%

Input parameters used to develop the comparison in Table 6.5 were as follows:

- a flow rate of 0.23 cfs (0.007 cms),

- a trench slope of 0.043 m/m,

- average Manning's $n = 0.014$ (average for entire movable bed study),

- $K_r = 0.036$ s/m, $\tau_c = 4.3$ Pa, and bulk density of sand, $\rho_b = 1.49$ g/sec.

Fabric discharge was neglected in analyzing movable-bed results because existing head-discharge relationships assume a constant flow depth relative to a point on the silt fence. Fabric flow rapidly decreased in movable-bed tests with significant scour. Fabric discharge became insignificant as the depth of flow

61

approached the depth of scour in the trench. A comparison of fabric discharge relative to flow in the trench for the fixed-bed study is provided as evidence of the influence of fabric discharge for various trench slopes. Figure 6.8 below indicates that fabric discharge was observed to be less than 0.8 percent of the flow in the trench for all conditions tested in the laboratory study.

Figure 6.8: Plot of relative fabric discharge for all test conditions

Relative Fabric Flow as a Function of Trench Slope
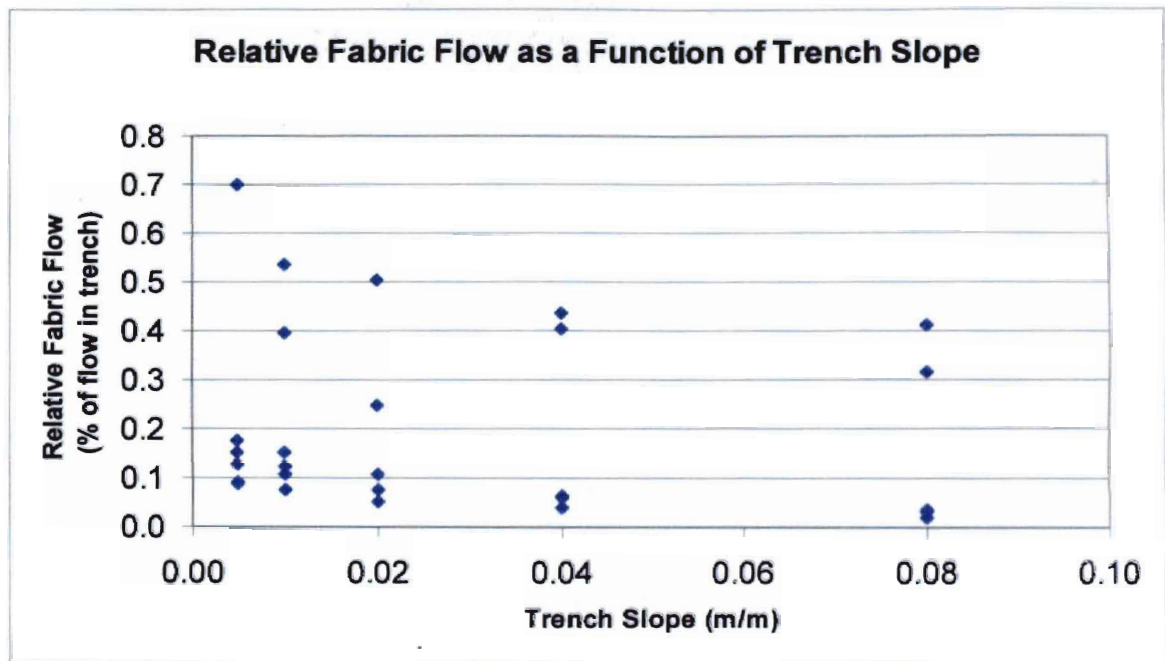
CHAPTER 7

SUMMARY AND CONCLUSIONS

7.1 Summary

Sediment loads in runoff from construction sites are significantly greater than those of agricultural lands and forested areas. During a short period of time, construction sites can contribute more sediment to streams than can be deposited naturally during several decades. The resulting situation, and the contribution of other pollutants from construction sites, can cause physical, chemical, and biological harm to aquatic ecosystems (USEPA, 1995). Silt fence is one of many methods available for curtailing sediment-laden runoff from construction areas, and it has proven to be an integral component of erosion prevention and sediment control plans in most municipalities.

Acceptable performance of silt fence was defined as the ability to effectively trap sediment on a construction site without experiencing undercutting or overtopping failure. The primary objective of this specific study was to evaluate the hydraulic performance of silt fence and the processes of undercutting for a range of trench slopes and concentrated flow conditions in a laboratory flume. An additional purpose of this study was to develop a process-based model for predicting the erosion of trench backfill material that occurs when a segment of silt fence functions as a flow diverting structure and converts overland flow into concentrated flow.

The variables contributing to the performance of a silt fence system were simulated with a mathematical model, which included routines for estimating the

63

physical processes of overland flow, spatially varied channel flow, and sediment transport. A silt fence system was conceptualized as a porous structure that collects runoff from a small drainage generating sediment-laden runoff. An experimental apparatus was designed and constructed to study flow along a silt fence trench with both non-erodible and erodible bed surfaces. A range of flow and slope conditions were tested, and the results were compared to the predictions generated with the process-based model.

7.2 Conclusions

Predicted depths of flow correlated well with observed depths of flow, but fabric discharge measurements did not follow the expected head-discharge relationship developed by Britton (2000). This was most likely a result of using the same piece of silt fence for the entire study, whereas Britton (2000) results were based on using a new piece of fabric for each flow test. One possible technique for correcting the flow prediction equation is to add a head loss term associated with flow velocity along a segment of filter fabric. This would require further investigation and analysis beyond the scope of this study. The evidence presented in this study suggests that silt fence that has been exposed to lake water discharges approximately one third of the flow that a new silt fence would discharge at a given head.

The issue of fabric tightness and its effects on the head-discharge relationship was considered beyond the scope of this study. Although tighter fabric may allow water to pass more freely than sagging fabric, the relationship is probably opposite. That is, discharge is most likely reduced when silt fence is

secured in a taut position as compared to sagging fabric. The woven configuration of fabric filaments is inherently flexible and allows the force of water to stretch and pass through openings when the filaments are not stretched. Consequently, a tightly stretched section of silt fence would have a smaller effective opening area when compared to a less tightly stretched section of the same fabric.

Predicted detachment rates were reasonably close to the measured detachment rates for both detachment capacity, Dc, based on the shear excess relationship and for actual detachment, Dr, or the detachment that accounts for the influence of transport capacity. Fabric discharge decreased significantly as the depth of flow approached the depth of scour in the trench.

7.3 Recommendations for Future Research

The laboratory study was designed to simulate an entrenched silt fence installed in a controlled environment. Certain assumptions were made to facilitate mathematical simulations of the silt fence system. For example, the trench was constructed with rectangular geometry to simplify measurements of flow depth and downward rate of scour. The silt fence was secured as taut as possible to ensure a rectangular cross section of flow, and plastic ties were evenly spaced along the vertical steel posts. The plastic ties should have only been used above the lower six inches of the steel posts, and it is also recommended that future tests should use silt fence that is not pre-attached to wooden posts since removing the fabric from the staples in the wood creates holes that interfere with fabric discharge.

More tests should be performed at a zero-slope setting to compare fabric discharge for new silt fence and silt fence that has experienced certain durations of flow. Exposing a piece of silt fence to distilled water and comparing its hydraulic performance to a silt fence exposed to lake water would provide a better understanding of the effects of micro plugging. Fabric tightness issues could be evaluated independently. The influences of fabric tightness on the head-discharge relationship should be considered when approximating effective opening area in the modified orifice equation for fabric flow.

The modeling framework developed and evaluated in this study should be refined to consider more accurate representations of the processes that impact silt fence performance. For example, actual failures of silt fence should be carefully monitored to ascertain the most important factors involved in various modalities of failure. The performance of silt fence under field conditions should be studied in carefully controlled experiments. Results of laboratory studies and field studies could then be used to develop site-specific design guidelines.

The results of the movable-bed study could be used to create design standards based on highly erodible trench backfill conditions. Such design standards would consider site-specific runoff for a 10 year, 24 hour design storm, and the mathematical model would be used to determine the maximum allowable trench length for a given fence slope and peak flow. The backfill material should be of adequate depth to prevent scouring of the top half for a 30-minute duration of the peak flow. Low resistance to erosion should be assumed for the trench backfill material unless compaction standards are developed and strictly

enforced. Additional experiments and analysis of data would help lead to the development of design criteria for allowable slope and trench length based on a range of soil conditions using soil characteristics from the WEPP database.

In summary, the existing experimental equipment should be modified to further evaluate the effects of prior flow and fabric tightness on the head-discharge relationship of silt fence. Field tests of silt fence in a controlled environment would provide valuable information on failure processes. The mathematical model should be adapted to more accurately predict fabric discharge for a wider a range of conditions, and further observation of processes related to silt fence failure should be considered in future model development. The modeling framework proposed in this study should ultimately be useful in developing silt fence design and installation criteria that is applicable and enforceable under all conceivable conditions encountered on construction sites.

BIBLIOGRAPHY

Alonso, C.V., W.H. Neibling and G.R. Foster. 1981. Estimating sediment transport capacity in watershed modeling. *Transactions of the American Society of Agricultural Engineers (ASAE).* 24(5):1211-1226.

Amoco Fabrics and Fibers Company. 2002. *ProPex 2130 Silt Fence Minimum Average Roll Values.* Amoco Fabrics and Fibers Co., Austell, GA.

ASTM Annual Book of Standards. 2003. D6462. *Standard Practice for Silt Fence Installation.* ASTM Vol. 04.09: West Conshohocken, PA.

Barr Engineering Company. 2001. *Minnesota Urban Small Sites BMP Manual.* Minneapolis, MN.

Barrett, M.E., J.E. Kearney, T.G. McCoy, J.F. Malina, R.J. Charbeneau, and G.H. Ward. 1995. An evaluation of the performance of geotextiles for temporary sediment control. Austin, TX: Center for Research in Water Resources, College of Engineering, The University of Texas at Austin.

Barfield, B. J. and J.C. Hayes. 1992. *Unpublished Results of Field Evaluation of Sediment Controls in South Carolina Construction Operations.* Biosystems and Agricultural Engineering, Oklahoma State University, Stillwater, OK.

Barfield, B. J. and J.C. Hayes. 1999. *Unpublished Results of Field Evaluation of Sediment Controls in Louisville, KY Construction Operations.* Biosystems and Agricultural Engineering, Oklahoma State University, Stillwater, OK.

Barfield, B. J., J.C. Hayes, A.W. Fogle, and K.A. Kranzler. 1996. "The SEDIMOT III – Model of Watershed Hydrology and Sedimentology," *Proceedings of Fifth Federal Interagency Sedimentation Conference,* Las Vegas, NV.

Barfield, B.J., J.C. Hayes, A.W. Fogle, M.R. Lindley, and D.E. Storm. 1994. Development Report for SEDIMOT III-Version 1. South Carolina Coastal Council. Charleston, SC.

Britton, S.L. 2000. Performance evaluation of silt fences for controlling sediment release. M.S. thesis. Biosystems Engineering Dept., Oklahoma State University, Stillwater, OK.

Brown, L.C., M.A. Nearing, G.R. Foster. 1989. Evaluating erosion parameters for a highly erosive soil using a modern erosion prediction model, Paper No. 89-2146. ASAE St. Joseph, MI.

Center for Watershed Protection (CWP). 2001. Stormwater manager's resource. Available at: http://stormwatercenter.net. Accessed: November 7, 2001.

Chow, V.T. 1959. "Open Channel Hydraulics." McGraw-Hill, New York.

Civil Engineering Research Foundation (CERF). 2001. *Environmental Technology Verification Report for Installation of Silt Fence Using the Tommy Static Slicing Method.* ASCE Environmental Technology Evaluation Center (EvTEC), CERF Report: #40565

Crebbin, C. 1988. "Laboratory evaluation of geotextile performance in silt fence applications using a subsoil of glacial origin." Master's Report, University of Washington

DSC, 1998. Strengthening silt fence. *Feature article from Watershed Protection Techniques.* Article 56, 2(3): pp. 424-428. Center for Watershed Protection, 8391 Main Street, Ellicott City, MD 21043. (www.cwp.org)

Elliott, W.J., A.M. Liebenow, J.M. Laflen, and K.D. Kohl. 1989. A compendium of soil erodibility data from wepp cropland soil field erodibility experiments 1987 & 1988. NSERL Report No. 3. The Ohio State University & USDA ARS.

Federal Highway Administration (FHWA). 1998. *Geosynthetic Design and Construction Guidelines Participant Handbook.* National Highway Institue, McLean, MA.

Fisher, L.S. and A.R. Jarrett. 1984. Sediment retention efficiency of synthetic filter fabrics. *Transactions of ASAE* 27(2):429-436.

Foster, G.R. and L.D. Meyer. 1972. Mathematical simulation of upland erosion by fundamental erosion mechanics. In "Proceedings, Sediment-Yield Workshop," USDA Sedimentation Laboratory, Oxford, Mississippi. pp. 190-207.

Foster, G.R. 1982. Modeling the erosion process. In "Hydrologic Modeling of Small Watersheds" (C.T. Haan, ed.) Monograph No. 5. ASAE, St. Joseph, MI.

Foster, G.R. and L.J. Lane. 1983. Erosion by concentrated flow in farm fields. In "Proceedings, D.B. Simons Symposium on Erosion and Sedimentation," Colorado State University, Ft. Collins, CO, pp. 9.65-9.82.

Foster, G.R., R.A. Young, and W.H. Neibling. 1985. Sediment composition for nonpoint source pollution analyses. *Trans. ASAE* 28(1):133-146.

Geosynthetic Materials Association (GMA), 2001. Handbook of Geosynthetics. Accessed on May 1, 2003 at http://www.gmanow.com/pdf/GMAHandbook_v002.pdf.

Haan, C.T., B.J. Barfield, and J.C. Hayes. 1994. *Design Hydrology and Sedimentology for Small Catchments.* San Diego, Academic Press, Inc.

Hayes, J. C. and B.J. Barfield. 1995. "Engineering Aids and Design Guidelines for Control of Sediment in South Carolina". In *South Carolina Stormwater and Sediment Control Handbook for Land Disturbance Activities.* South Carolina Department of Health and Environmental Control. Columbia, SC.

Herzog, M.J. Harbor, K McClintock, J. Law, and K. Bennett. 2000. Are green lots worth more than brown lots? An economic incentive for erosion control on residential developments. *J. of Soil and Water Conservation* 55: 43-48.

Horner, R.R., J. Guedry and M.H. Kortenhof. 1990. Improving the Cost Effectiveness of Highway Construction Site Erosion and Pollution Control. *Washington State Transportation Center and the Federal Highway Administration. Seattle, WA. 79 pp.*

Jiang, N. 1997. Hydraulic performance of porous sediment control structures. Ph.D. diss., Agricultural Engineering Dept., University of Illinois, Urbana-Champaign.

Koerner, R. M. 1990. "Designing with Geosynthetics," Prentice Hall. Englewood Cliffs, NJ.

Kouwen, N. 1990. Silt fences to control sediment movement on construction sites, MAT-90-03." The Research and Development Branch, Ontario Ministry of Transportation.

Lindley, M., B. J. Barfield, J. Ascough, B. N. Wilson, and E. Stevens. 1998. "The Surface Impoundment Element for WEPP". *Transactions of the American Society of Agricultural Engineers (ASAE).* 41(3):555-564.

Lu, J.Y., G.R. Foster, and R.E. Smith. 1987. Numerical simulation of dynamic erosion in a ridge-furrow system. *Transactions of ASAE* 30(4):969-976.

McPherson, M.B. 1969. Some notes on the rational method of storm drain design, Technical memorandum No. 6, ASCE Urban Water Resource Research Program. ASCE, New York.

Meyer, L.D. and W.H. Wischmeier. 1969. Mathematical simulation of the process of soil erosion by water. *Transactions of the American Society of Agricultural Engineers (ASAE).* 12(6):754-758.

Natural Resource Conservation Service (NRCS), formerly Soil Conservation Service (SCS). 1985. "Hydrology," Sect. 4, Nat. Res. Cons. Service (NRCS) National Engineering Handbook. U.S. Department of Agriculture, Washington D.C.

Natural Resource Conservation Service (NRCS). 1986. Urban hydrology for small watersheds, Technical release No. 55. Nat. Res. Cons. Service, U.S. Department of Agriculture, Washington D.C.

Natural Resource Conservation Service (NRCS). 2000. Urban Construction Sediment Control Manual. Caribbean Area Puerto Rico and the US Virgin Islands NRCS, San Juan, PR.

Nearing, M.A., G.R. Foster, L.J. Lane, and S.C. Finkner. 1989. A process-based soil erosion model for USDA-Water Erosion Prediction Project technology. *Trans. ASAE* 32(5): 1587-1593.

Nearing, M.A., L.J. Lane, E.E. Alberts, and J.M. Laflen. 1990. Prediction technology for soil erosion by water: Status and research needs. Soil Science Soc. of Am. J. 54(6): 1702-1711.

Nearing, M.A., L.J. Lane, and V.L. Lopes. 1994. Modeling Soil Erosion in *Soil Erosion Research Methods*. R. Lal, Ed. St. Lucie Press, Delray Beach, FL.

Nearing, M.A., L.D. Norton, D.A. Bulgakov, G.A. Larionov, L.T. West, and K.M. Dontsova. 1997. Hydraulics and erosion in eroding rills. Water Resources Research 33(4): 865-876

Richardson, G.N. and P. Middlebrooks. 1991. A simplified design method for silt fences. In Proc. Geosynthetics Conf., pp 879-888. Atlanta, GA.

Rubin, D.K. and W.J. Angelo. 2001. Regulating runoff: government tightens grip on construction sites to limit stormwater impact on U.S. water quality. *Engineering News-Record*. October 15, 2001. v247(16): 40-42.

Smolen, M.D., D.W. Miller, L.C. Wyall, J. Lichthardt, and A.L. Lanier. 1988. *Erosion and Sediment Control Planning and Design Manual*. North Carolina Sedimentation Control Commission and North Carolina Dept. of Natural Resources and Community Development, Raleigh, NC.

Sprague, C.J. 2002. *A Field Study: The Inspection of Randomly Selected Silt Fence Installations Around the United States*. TRI Environmental, Inc. Austin, TX.

Storm, D.E. 1991. Modeling dynamic rill networks from random surfaces on moderate slopes. Ph.D. diss. Agricultural Engineering Dept., The University of Kentucky, Lexington, KY.

United States Department of Transportation (USDOT). 1995. *Best Management Practices for Erosion and Sediment Control*. Report No. FHWA-FLP-94-005. Eastern Federal Lands Highway Design, U.S Department of Transportation, Sterling, VA.

United States Environmental Protection Agency (USEPA). 2002. *Development Document for Proposed Effluent Guidelines and Standards for the Construction and Development Category*. USEPA, Office of Water (4303T), EPA-821-R-02-007.

United States Environmental Protection Agency (USEPA). 1998. *The Quality of Our Nation's Waters, A Summary of the National Water Quality Inventory: 1998 Report to Congress*. USEPA (305B), EPA841-S-00-001.

United States Environmental Protection Agency (USEPA). 1995. *Erosion, Sediment, and Runoff Control for Roads and Highways*. USEPA, Office of Water (4503F), EPA-841-F-95-008d.

United States Environmental Protection Agency (USEPA). 1992. *Storm Water Management for Construction Activities: Developing Pollution Prevention*

Plans and Best Management Practices. EPA 832-R-92-005. USEPA, Office of Water, Washington, DC.

Watson, D. A., J. M. Laflen, and T. G. Franti. 1986. Estimating ephemeral gully erosion, Paper No. 86-2020. American Society of Agricultural Engineers, St. Joseph, MI.

Williams, J. R., and A. D. Brendt. 1972. Sediment yield computed with Universal Equation. Proc. Am. Soc. Civil Eng. 98(HY12):2087-2098

Water Pollution Control Federation (WPCF). 1969. Design and construction of sanitary and storm sewers. Manual of practice 9. (ASCE Manual of Eng. Practice No. 37) WPCF, 3900 Wisconsin Ave., Washington, DC.

Wilson, B.N. 1993. Development of a Fundamentally Based Detachment Model, *Transactions of ASAE* 36(4):1105-1114.

Wischmeier, W.H. and D.D. Smith. 1978. Predicting rainfall erosion losses—A guide to conservation planning, Agricultural Handbook No. 537. U.S. Department of Agriculture, Washington, DC.

Wyant, D.C. 1980. Evaluation of filter fabrics used as silt fences. Charlottesville, VA: Virginia Highway and Transportation Research Council.

Yalin, Y.S. 1963. An expression for bed-load transportation. J. *Hyd. Div. Proc. ASCE* 89(HY3):221-250.

Yang, C.T. 1972. Unit stream power and sediment transport. J. *Hyd. Div. Proc. ASCE* 98(HY10):1805-1826.

Yang, C.T. 1973. Incipient motion and sediment transport. J. *Hyd. Div. Proc. ASCE* 98(HY10):1679-1704.

Zhang, G.-H., B.-Y. Liu, M.A. Nearing, C.-H. Huang, K.-L. Zhang. 2002. Soil detachment by shallow flow. *Transactions of ASAE* 45(2): 351-357.

APPENDICES

APPENDIX A

Procedures for Laboratory Tests

Preliminary Test Preparations

- Flow distribution was analyzed for a section of horizontal pipe with drilled orifices to determine proper spacing and pressure requirements.
- Geometric configuration of a simulated trench was selected and fabricated.
- Upstream and overland flow devices were connected to existing supply lines in a model building with a gravity flow water supply.
- Filter fence hydraulics testing apparatus with an adjustable-slope trench was constructed in a laboratory flume.
- Monitoring equipment such as a point gauge was mounted on rails that were secured to a steel framework along the test section.
- An H-flume with catch basin was installed downstream of the adjustable slope filter fence test channel and the control section of the H-flume was secured to the concrete floor and leveled.
- Inlet and outlet connections were sealed to the test channel using a flexible rubber liner.
- A clear acrylic channel extension was constructed and attached to the downstream end of the silt fence test section to allow visual monitoring of flow and sediment movement.
- Desired slope and flow settings were selected and randomized to determine the sequence of tests.

Fixed-bed Test Procedures

1. Point gauge support rails were leveled and bed slope was measured by taking point gauge readings at one-foot increments over the length of the test section.
2. Flow collection system consisting of ten five-gallon buckets was positioned next to filter fabric flow drains.
3. Orifice plate with manometer board was used to adjust upstream flow conditions.
4. Two minutes were allowed for flow stabilization before H-flume flow depth measurements were recorded.
5. Wetting the outer filter fabric surface in the test section broke surface tension.
6. Drain hoses were positioned to initiate fabric flow collection in buckets after noting the time.
7. Bed and water surface profiles were measured with a point gauge at one-foot stations over the length of the test section.
8. Drain hoses were removed from the fabric flow collection system, the time was noted, and volume of water in each bucket was measured.

Movable-bed Test Procedures

1. Small drain holes were drilled along the trench bottom.
2. Permeable geotextile liner was placed along the trench bottom.
3. Trench was filled with 1.1 ft of soil to allow for settling during consolidation.
4. Soil was saturated and drained to achieve uniform consolidation.
5. Soil density samples were collected upstream from test section.
6. Point gauge support rails were leveled along the test section.
7. Soil surface was graded to final level.
8. Bed profile was measured to determine required slope adjustment.
9. Slope setting was adjusted to achieve desired test slope.
10. Initial bed profile data was collected.
11. Desired flow was set using valve and manometer system.
12. The time flow entered trench was noted.
13. Manometer reading was checked.
14. End gate measurement was recorded.
15. Readings for depth of flow in H-flume were taken.
16. Sediment sample was collected.
17. Photograph was captured of flow in clear channel extension.
18. Water surface profile was measured.

Steps 9 through 14 were repeated at reasonable times for the duration of the test with a minimum of three repetitions.

APPENDIX B

Data Analysis for Fixed-Bed Study

Data Analysis for Tests with Upstream Flow Only

Label	Slope (m/m)	Upstream Flow (cfs)	(cms)	Fabric Flow (cfs)	(cms)	H-flume Flow (cfs)	(cms)	Av. Depth of Flow (ft)	(m)	V = Q/A (fps)	R (ft)	n	F	Bed Shear = γDS (lb/ft²)	(Pa)
0.5A1	0.005	0.175	0.005	0.0012	3.4E-05	0.173	0.0049	0.181	0.055	1.938	0.105	0.011	0.8	0.0565	2.70
0.5A2	0.005	0.175	0.005	0.0002	4.4E-06	0.172	0.0049	0.127	0.039	2.759	0.084	0.007	1.4	0.0396	1.89
0.5A3	0.005	0.175	0.005	0.0002	4.3E-06	0.171	0.0048	0.129	0.039	2.712	0.085	0.008	1.3	0.0403	1.93
0.5B1	0.005	0.350	0.010	0.0043	1.2E-04	0.340	0.0096	0.316	0.096	2.219	0.139	0.011	0.7	0.0985	4.72
0.5B2	0.005	0.350	0.010	0.0005	1.5E-05	0.342	0.0097	0.197	0.060	3.563	0.110	0.007	1.4	0.0613	2.94
0.5B3	0.005	0.350	0.010	0.0006	1.7E-05	0.342	0.0097	0.198	0.060	3.529	0.111	0.007	1.4	0.0619	2.96
01A1	0.01	0.175	0.005	0.0009	2.7E-05	0.176	0.0050	0.112	0.034	3.134	0.077	0.009	1.7	0.0696	3.33
01A2	0.01	0.175	0.005	0.0002	5.3E-06	0.174	0.0049	0.108	0.033	3.242	0.075	0.008	1.7	0.0673	3.22
01A3	0.01	0.175	0.005	0.0001	3.8E-06	0.174	0.0049	0.109	0.033	3.218	0.076	0.008	1.7	0.0679	3.25
01B1	0.01	0.350	0.010	0.0014	3.9E-05	0.346	0.0098	0.182	0.055	3.850	0.105	0.009	1.6	0.1135	5.44
01B2	0.01	0.350	0.010	0.0004	1.2E-05	0.338	0.0096	0.174	0.053	4.022	0.103	0.008	1.7	0.1086	5.20
01B3	0.01	0.350	0.010	0.0005	1.5E-05	0.343	0.0097	0.173	0.053	4.046	0.102	0.008	1.7	0.1080	5.17
02A1	0.02	0.176	0.005	0.0004	1.2E-05	0.176	0.0050	0.094	0.029	3.746	0.068	0.009	2.2	0.1169	5.60
02A2	0.02	0.175	0.005	0.0001	3.8E-06	0.173	0.0049	0.093	0.028	3.741	0.068	0.009	2.2	0.1167	5.59
02A3	0.02	0.175	0.005	0.0001	2.6E-06	0.175	0.0050	0.094	0.029	3.740	0.068	0.009	2.2	0.1168	5.59
02B1	0.02	0.350	0.010	0.0017	4.9E-05	0.345	0.0098	0.151	0.046	4.632	0.094	0.009	2.1	0.1887	9.04
02B2	0.02	0.350	0.010	0.0004	1.1E-05	0.350	0.0099	0.151	0.046	4.651	0.094	0.009	2.1	0.1879	9.00
02B3	0.02	0.350	0.010	0.0004	1.0E-05	0.343	0.0097	0.151	0.046	4.649	0.094	0.009	2.1	0.1879	9.00
04A1	0.04	0.175	0.005	0.0007	2.0E-05	0.177	0.0050	0.077	0.024	4.535	0.059	0.010	2.9	0.1925	9.22
04A2	0.04	0.175	0.005	0.0001	2.1E-06	0.173	0.0049	0.077	0.023	4.565	0.059	0.010	2.9	0.1914	9.16
04A3	0.04	0.175	0.005	0.0001	2.0E-06	0.173	0.0049	0.076	0.023	4.580	0.059	0.010	2.9	0.1907	9.13
04B1	0.04	0.350	0.010	0.0015	4.3E-05	0.345	0.0098	0.128	0.039	5.490	0.084	0.010	2.7	0.3183	15.25
04B2	0.04	0.350	0.010	0.0002	6.3E-06	0.347	0.0098	0.127	0.039	5.494	0.084	0.010	2.7	0.3180	15.23
04B3	0.04	0.350	0.010	0.0002	5.9E-06	0.343	0.0097	0.128	0.039	5.478	0.085	0.010	2.7	0.3190	15.28
08A1	0.08	0.175	0.005	0.0006	1.6E-05	0.177	0.0050	0.063	0.019	5.571	0.050	0.010	3.9	0.3135	15.01
08A2	0.08	0.175	0.005	0.0001	1.7E-06	0.177	0.0050	0.047	0.014	7.423	0.040	0.007	6.0	0.2352	11.27
08A3	0.08	0.175	0.005	0.0000	1.0E-06	0.179	0.0051	0.064	0.020	5.447	0.051	0.011	3.8	0.3207	15.36
08B1	0.08	0.350	0.010	0.0014	4.0E-05	0.348	0.0099	0.105	0.032	6.850	0.074	0.011	3.6	0.5256	25.17
08B2	0.08	0.350	0.010	0.0001	3.0E-06	0.347	0.0098	0.103	0.031	6.812	0.073	0.011	3.7	0.5131	24.58
08B3	0.08	0.350	0.010	0.0001	3.4E-06	0.344	0.0097	0.107	0.033	6.552	0.075	0.011	3.5	0.5333	25.54
10B1	0.1	0.350	0.010	0.0006	1.8E-05	0.345	0.0098	0.099	0.030	7.074	0.071	0.011	4.0	0.6180	29.60

Averages of triplets (repetitions of slope and flow settings)

Label	Slope (m/m)	Upstream Flow (cfs)	(cms)	Fabric Flow (cfs)	(cms)	H-flume Flow (cfs)	(cms)	Av. Depth of Flow (ft)	(m)	V = Q/A (fps)	R (ft)	n	F	Bed Shear = γDS (lb/ft²)	(Pa)
av0.5A	0.005	0.175	0.005	0.0005	1.4E-05	0.172	0.0049	0.146	0.044	2.470	0.091	0.009	1.2	0.045	2.18
av0.5B	0.005	0.350	0.010	0.0018	5.1E-05	0.341	0.0097	0.237	0.072	3.104	0.120	0.008	1.2	0.074	3.54
av01A	0.01	0.175	0.005	0.0004	1.2E-05	0.175	0.0050	0.109	0.033	3.198	0.076	0.008	1.7	0.068	3.27
av01B	0.01	0.350	0.010	0.0008	2.2E-05	0.342	0.0097	0.176	0.054	3.973	0.103	0.008	1.7	0.110	5.27
av02A	0.02	0.175	0.005	0.0002	6.2E-06	0.175	0.0049	0.094	0.029	3.742	0.068	0.009	2.2	0.117	5.59
av02B	0.02	0.350	0.010	0.0008	2.3E-05	0.346	0.0098	0.151	0.046	4.644	0.094	0.009	2.1	0.188	9.01
av04A	0.04	0.175	0.005	0.0003	8.1E-06	0.174	0.0049	0.077	0.023	4.560	0.059	0.010	2.9	0.192	9.17
av04B	0.04	0.350	0.010	0.0006	1.8E-05	0.345	0.0098	0.128	0.039	5.487	0.084	0.010	2.7	0.318	15.25
av08A	0.08	0.175	0.005	0.0002	6.2E-06	0.178	0.0050	0.058	0.018	6.147	0.047	0.009	4.6	0.290	13.86
av08B	0.08	0.350	0.010	0.0006	1.6E-05	0.346	0.0098	0.105	0.032	6.671	0.074	0.011	3.6	0.524	25.10

Standard Deviations of each triplet

Label	Slope (m/m)	Upstream Flow (cfs)	(cms)	Fabric Flow (cfs)	(cms)	H-flume Flow (cfs)	(cms)	Av. Depth of Flow (ft)	(m)	V = Q/A (fps)	R (ft)	n	F	Bed Shear = γDS (lb/ft²)	(Pa)
sd0.5A	0.0000	0.0002	0.0002	0.0005	0.0000	0.0007	0.0000	0.0251	0.0076	0.3765	0.0096	0.0016	0.2575	0.0078	0.3743
sd0.5B	0.0000	0.0000	0.0000	0.0018	0.0001	0.0010	0.0000	0.0557	0.0170	0.6259	0.0138	0.0022	0.3350	0.0174	0.8323
sd01A	0.0000	0.0001	0.0001	0.0004	0.0000	0.0007	0.0000	0.0016	0.0005	0.0464	0.0008	0.0002	0.0367	0.0010	0.0466
sd01B	0.0000	0.0000	0.0000	0.0004	0.0000	0.0033	0.0001	0.0040	0.0012	0.0874	0.0014	0.0003	0.0549	0.0025	0.1181
sd02A	0.0000	0.0003	0.0003	0.0002	0.0000	0.0010	0.0000	0.0024	0.0000	0.0006	0.0008	0.0001	0.0051		
sd02B	0.0000	0.0000	0.0000	0.0006	0.0000	0.0031	0.0001	0.0003	0.0001	0.0084	0.0001	0.0000	0.0058	0.0004	0.0169
sd04A	0.0000	0.0000	0.0000	0.0003	0.0000	0.0018	0.0001	0.0003	0.0001	0.0186	0.0002	0.0001	0.0173	0.0007	0.0351
sd04B	0.0000	0.0000	0.0000	0.0006	0.0000	0.0017	0.0000	0.0002	0.0000	0.0069	0.0001	0.0001	0.0050	0.0004	0.0186
sd08B	0.0000	0.0000	0.0000	0.0002	0.0000	0.0008	0.0000	0.0076	0.0024	0.9035	0.0052	0.0018	1.0259	0.0387	1.8533
sd08B	0.0000	0.0000	0.0000	0.0006	0.0000	0.0019	0.0001	0.0017	0.0005	0.1070	0.0008	0.0003	0.0872	0.0083	0.3982

Data Analysis for Tests with Upstream Flow and Overland Flow

Test Label	Slope (m/m)	Upstream Flow (cfs)	Upstream Flow (cms)	P (pipe)	Overland Flow (cfs)	Overland Flow (cms)	Fabric Flow Q, cfs	Fabric Flow Q, cms	H-flume Flow Q, cfs	H-flume Flow Q, cms	Av. Depth of Flow (ft)	Av. Depth of Flow (m)	V (fps)	R (ft)	n	F	Bed Shear = γDS (lb/ft²)	Bed Shear = γDS (Pa)
0.5A1	0.005	0.175	0.005	0.5 psi	0.076	0.0021	0.0029	8E-05	0.254	0.0072	0.291	0.089	1.20	0.135	0.021	0.4	0.091	4.36
0.5A2	0.005	0.175	0.005	0.5 psi	0.073	0.0021	0.0011	3E-05	0.249	0.0070	0.265	0.081	1.32	0.129	0.020	0.5	0.083	3.96
0.5A3	0.005	0.175	0.005	0.5 psi	0.074	0.0021	0.0007	2E-05	0.249	0.0071	0.276	0.084	1.27	0.131	0.021	0.4	0.086	4.13
0.5B1	0.005	0.350	0.010	0.5 psi	0.060	0.0017	0.0069	2E-04	0.417	0.0118	0.411	0.125	1.70	0.155	0.016	0.5	0.128	6.14
0.5B2	0.005	0.350	0.010	0.5 psi	0.052	0.0015	0.0020	6E-05	0.404	0.0114	0.381	0.116	1.84	0.151	0.016	0.5	0.119	5.69
0.5B3	0.005	0.350	0.010	0.5 psi	0.055	0.0015	0.0017	5E-05	0.406	0.0115	0.383	0.117	1.83	0.151	0.016	0.5	0.120	5.73
01A1	0.010	0.175	0.005	0.5 psi	0.080	0.0023	0.0034	1E-04	0.258	0.0073	0.236	0.072	1.49	0.121	0.025	0.5	0.147	7.05
01A2	0.010	0.175	0.005	0.5 psi	0.076	0.0021	0.0006	2E-05	0.251	0.0071	0.220	0.067	1.59	0.117	0.022	0.6	0.137	6.58
01A3	0.010	0.175	0.005	0.5 psi	0.076	0.0021	0.0005	1E-05	0.251	0.0071	0.149	0.045	4.70	0.093	0.007	2.1	0.093	4.45
01B1	0.010	0.350	0.010	0.5 psi	0.069	0.0020	0.0052	1E-04	0.424	0.0120	0.332	0.101	2.10	0.143	0.019	0.6	0.207	9.94
01B2	0.010	0.350	0.010	0.5 psi	0.072	0.0020	0.0010	3E-05	0.423	0.0120	0.280	0.085	2.50	0.132	0.015	0.8	0.175	8.36
01B3	0.010	0.350	0.010	0.5 psi	0.060	0.0017	0.0011	3E-05	0.411	0.0116	0.287	0.087	2.44	0.134	0.016	0.8	0.179	8.57
02A1	0.020	0.176	0.005	0.5 psi	0.083	0.0024	0.0015	4E-05	0.260	0.0074	0.151	0.046	2.32	0.094	0.019	1.1	0.189	9.04
02A2	0.020	0.175	0.005	0.5 psi	0.083	0.0023	0.0002	6E-06	0.258	0.0073	0.149	0.045	2.35	0.093	0.018	1.1	0.186	8.92
02A3	0.020	0.175	0.005	0.5 psi	0.080	0.0023	0.0002	7E-06	0.256	0.0072	0.151	0.046	2.32	0.094	0.019	1.1	0.188	9.03
02B1	0.020	0.350	0.010	0.5 psi	0.075	0.0021	0.0022	6E-05	0.427	0.0121	0.203	0.062	3.45	0.112	0.014	1.4	0.253	12.13
02B2	0.020	0.350	0.010	0.5 psi	0.069	0.0020	0.0006	2E-05	0.420	0.0119	0.201	0.061	3.48	0.112	0.014	1.4	0.251	12.04
02B3	0.020	0.350	0.010	0.5 psi	0.072	0.0020	0.0007	2E-05	0.423	0.0120	0.199	0.061	3.52	0.111	0.014	1.4	0.249	11.90
04A1	0.040	0.176	0.005	0.5 psi	0.083	0.0023	0.0013	4E-05	0.260	0.0074	0.115	0.035	3.04	0.079	0.018	1.6	0.288	13.78
04A2	0.040	0.175	0.005	0.5 psi	0.083	0.0023	0.0001	4E-06	0.258	0.0073	0.117	0.036	2.99	0.080	0.018	1.5	0.292	13.99
04A3	0.040	0.175	0.005	0.5 psi	0.082	0.0023	0.0001	3E-06	0.257	0.0073	0.111	0.034	3.14	0.077	0.017	1.7	0.278	13.31
04B1	0.040	0.352	0.010	0.5 psi	0.070	0.0020	0.0036	1E-04	0.426	0.0121	0.160	0.049	4.39	0.098	0.014	1.9	0.401	19.18
04B2	0.040	0.350	0.010	0.5 psi	0.064	0.0018	0.0003	9E-06	0.414	0.0117	0.175	0.053	4.01	0.103	0.016	1.7	0.436	20.89
04B3	0.040	0.350	0.010	0.5 psi	0.067	0.0019	0.0003	9E-06	0.417	0.0118	0.165	0.050	4.24	0.099	0.015	1.8	0.412	19.75
08A1	0.080	0.175	0.005	0.5 psi	0.082	0.0023	0.0008	2E-05	0.258	0.0073	0.087	0.027	4.01	0.065	0.017	2.4	0.436	20.87
08A2	0.080	0.176	0.005	0.5 psi	0.076	0.0021	0.0001	3E-06	0.251	0.0071	0.085	0.026	4.12	0.064	0.016	2.5	0.425	20.36
08A3	0.080	0.175	0.005	0.5 psi	0.071	0.0020	0.0000	1E-06	0.246	0.0070	0.084	0.026	4.17	0.063	0.016	2.5	0.418	20.04
08B1	0.080	0.350	0.010	0.5 psi	0.077	0.0022	0.0017	5E-05	0.429	0.0121	0.129	0.039	5.43	0.085	0.015	2.7	0.644	30.85
08B2	0.080	0.350	0.010	0.5 psi	0.074	0.0021	0.0001	3E-06	0.424	0.0120	0.118	0.036	5.93	0.080	0.013	3.0	0.589	28.22
08B3	0.080	0.350	0.010	0.5 psi	0.066	0.0019	0.0002	4E-06	0.416	0.0118	0.127	0.039	5.52	0.084	0.015	2.7	0.633	30.32
10B1	0.100	0.350	0.010	0.5 psi	0.073	0.0021	0.0006	2E-05	0.424	0.0120	0.118	0.036	5.96	0.080	0.015	3.1	0.733	35.11

Averages of triplets (repetitions of slope and flow settings)

Test Label	Slope (m/m)	Upstream (cfs)	Upstream (cms)		Overland (cfs)	Overland (cms)	Fabric Q, cfs	Fabric Q, cms	H-flume Q, cfs	H-flume Q, cms	Av. Depth (ft)	Av. Depth (m)	V (fps)	R (ft)	n	F	Bed Shear (lb/ft²)	Bed Shear (Pa)
av0.5A	0.005	0.175	0.005		0.07	0.0021	0.0016	4.5E-05	0.2507	0.0071	0.278	0.085	1.26	0.131	0.021	0.4	0.087	4.15
av0.5B	0.005	0.350	0.010		0.06	0.0016	0.0035	1.0E-04	0.4091	0.0116	0.392	0.119	1.79	0.153	0.016	0.5	0.122	5.85
av01A	0.01	0.175	0.005		0.08	0.0022	0.0015	4.2E-05	0.2535	0.0072	0.202	0.061	2.59	0.111	0.018	1.1	0.126	6.03
av01B	0.01	0.350	0.010		0.07	0.0019	0.0024	6.9E-05	0.4194	0.0119	0.300	0.091	2.35	0.136	0.017	0.8	0.187	8.90
av02A	0.02	0.175	0.005		0.08	0.0023	0.0007	1.9E-05	0.2578	0.0073	0.151	0.046	2.33	0.094	0.019	1.1	0.188	9.00
av02B	0.02	0.350	0.010		0.07	0.0020	0.0012	3.3E-05	0.4232	0.0120	0.201	0.061	3.48	0.111	0.014	1.4	0.251	12.02
av04A	0.04	0.175	0.005		0.08	0.0023	0.0005	1.5E-05	0.2581	0.0073	0.115	0.035	3.06	0.079	0.018	1.6	0.286	13.69
av04B	0.04	0.351	0.010		0.07	0.0019	0.0014	4.0E-05	0.4192	0.0119	0.167	0.051	4.21	0.100	0.015	1.8	0.416	19.94
av08A	0.08	0.175	0.005		0.08	0.0022	0.0003	9.0E-06	0.2517	0.0071	0.085	0.026	4.10	0.064	0.016	2.5	0.426	20.42
av08B	0.08	0.350	0.010		0.07	0.0020	0.0007	1.9E-05	0.4230	0.0120	0.125	0.038	5.63	0.083	0.014	2.8	0.622	29.80

Standard Deviations of each triplet

Test Label	Slope (m/m)	Upstream (cfs)	Upstream (cms)		Overland (cfs)	Overland (cms)	Fabric Q, cfs	Fabric Q, cms	H-flume Q, cfs	H-flume Q, cms	Av. Depth (ft)	Av. Depth (m)	V (fps)	R (ft)	n	F	Bed Shear (lb/ft²)	Bed Shear (Pa)
sd0.5A	0.0000	0.0001	0.0000		0.0016	0.0000	0.0012	0.0000	0.0027	0.0001	0.0132	0.0040	0.0594	0.0030	0.0006	0.0299	0.0041	0.1977
sdv0.5B	0.0000	0.0001	0.0000		0.0040	0.0001	0.0029	0.0001	0.0068	0.0002	0.0165	0.0050	0.0733	0.0025	0.0002	0.0308	0.0051	0.2458
sd01A	0.0000	0.0003	0.0000		0.0022	0.0001	0.0016	0.0000	0.0041	0.0001	0.0463	0.0141	1.8279	0.0151	0.0099	0.9120	0.0289	1.3851
sd01B	0.0000	0.0001	0.0000		0.0065	0.0002	0.0024	0.0001	0.0073	0.0002	0.0286	0.0087	0.2141	0.0058	0.0021	0.1023	0.0178	0.8548
sd02A	0.0000	0.0003	0.0000		0.0015	0.0000	0.0008	0.0000	0.0023	0.0001	0.0011	0.0003	0.0155	0.0004	0.0002	0.0110	0.0014	0.0674
sd02B	0.0000	0.0001	0.0000		0.0028	0.0001	0.0009	0.0000	0.0036	0.0001	0.0019	0.0006	0.0323	0.0006	0.0002	0.0191	0.0024	0.1130
sd04A	0.0000	0.0003	0.0000		0.0005	0.0000	0.0007	0.0000	0.0014	0.0000	0.0029	0.0009	0.0767	0.0014	0.0006	0.0603	0.0072	0.3447
sd04B	0.0000	0.0012	0.0000		0.0030	0.0001	0.0019	0.0001	0.0058	0.0002	0.0073	0.0022	0.1923	0.0026	0.0010	0.1218	0.0182	0.8701
sd08A	0.0000	0.0003	0.0000		0.0055	0.0002	0.0004	0.0000	0.0058	0.0002	0.0017	0.0005	0.0856	0.0010	0.0005	0.0766	0.0087	0.4170
sd08B	0.0000	0.0001	0.0000		0.0055	0.0002	0.0009	0.0000	0.0063	0.0002	0.0058	0.0018	0.2692	0.0026	0.0010	0.2028	0.0290	1.3912

APPENDIX C

Particle Size Distribution of Bed Material

| Soil C		Sample No.			Samples were taken from the west bin of the concrete sand material at the ARS Hydraulics Laboratory.			
		1	2	3				
Total Sample (g)		115.01	115.59	115.47				
Sieve No.	Size (mm)	Mass Retained (g)			Mean (g)	Std. Dev.	% Finer	Size (mm)
4	4.750	2.19	2.43	1.22	1.95	0.64	98.3	4.750
10	2.000	5.64	5.58	4.53	5.25	0.62	93.7	2.000
20	0.850	26.07	30.08	27.51	27.89	2.03	69.5	0.850
40	0.425	53.79	54.49	53.4	53.89	0.55	22.6	0.425
60	0.250	20.71	18.33	19.6	19.55	1.19	5.6	0.250
140	0.106	5.27	4.4	7.51	5.73	1.60	0.6	0.106
200	0.075	0.28	0.31	0.75	0.45	0.26	0.2	0.075
PAN	0.000	0.18	0.2	0.4	0.26	0.12	0.0	0.000
Total Retained (g)		114.13	115.82	114.92	114.96			

Particle Size Distribution for Bed Material
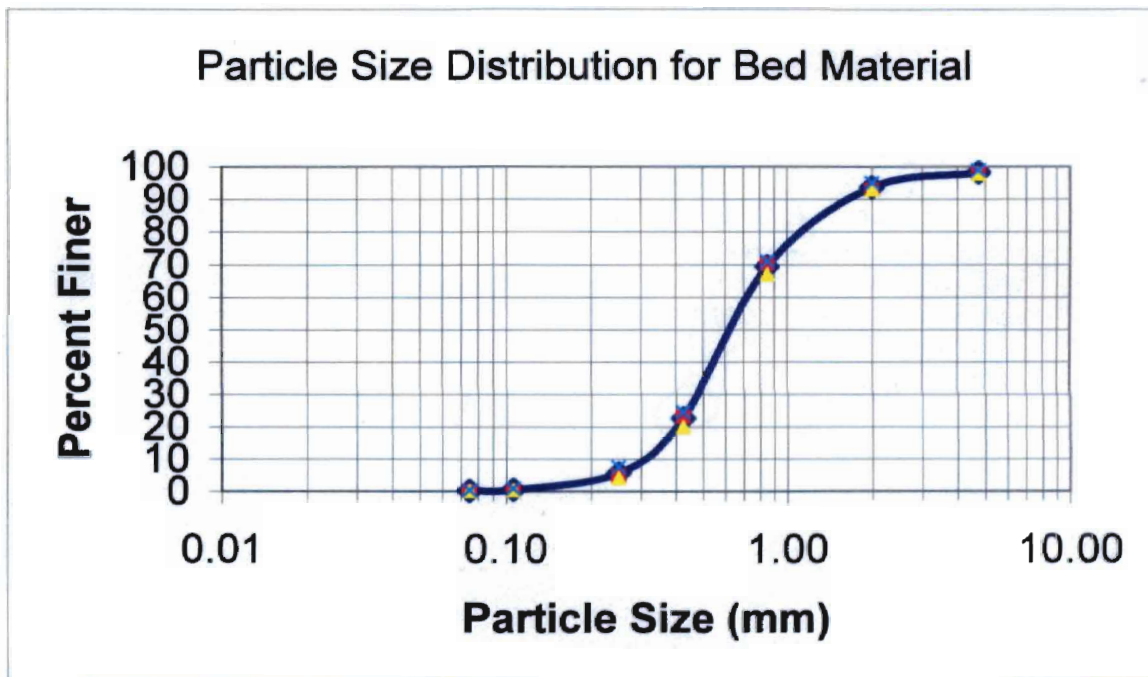
APPENDIX D

Plots of Initial and Final Bed Profiles

Test No. 1, Bed Profiles for 1.0% Initial Slope
Q = 0.175 cfs and Duration of Test = 73 min
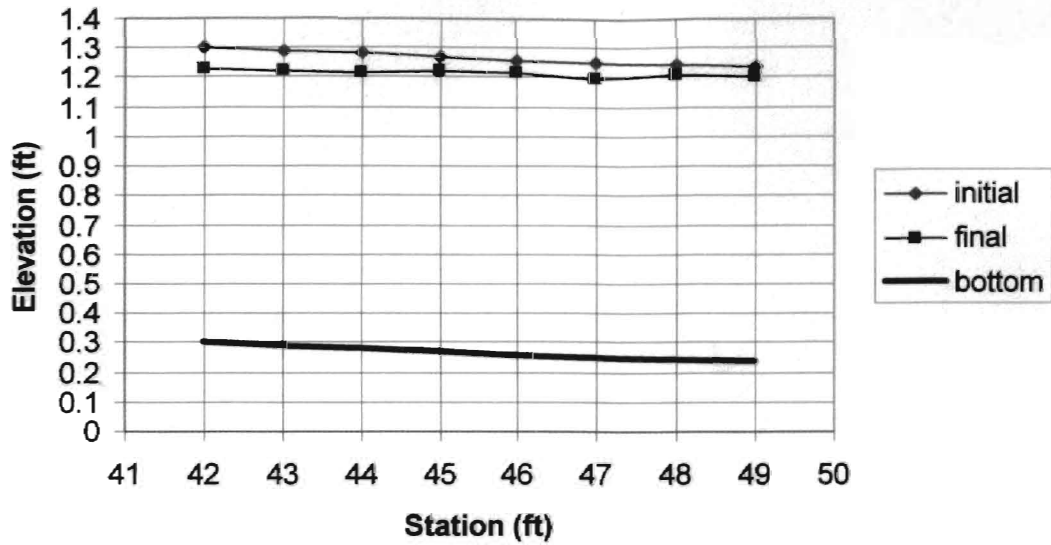
Test No. 2, Bed Profiles for 2.4% Initial Slope
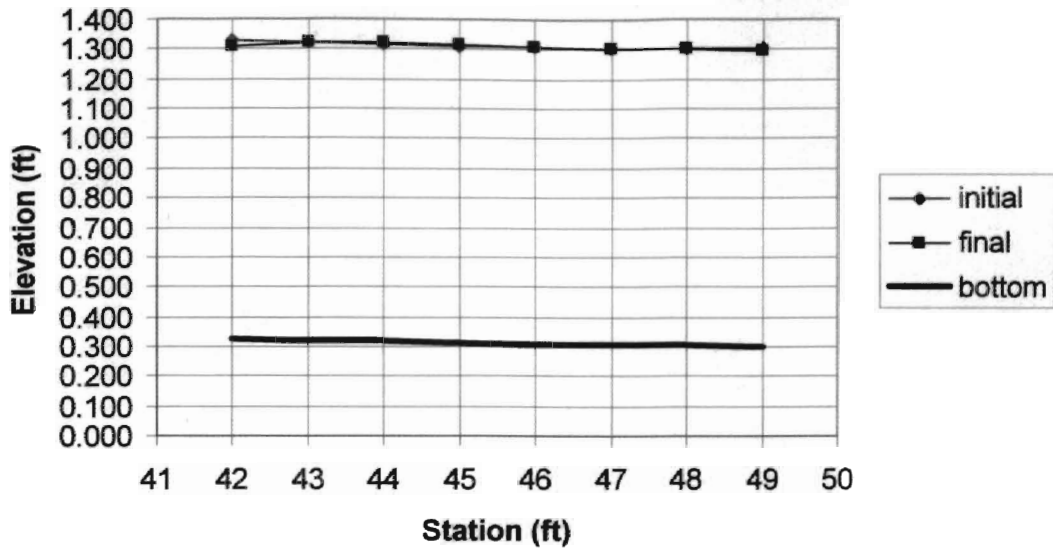Q = 0.175 cfs and Duration of Test = 27 min
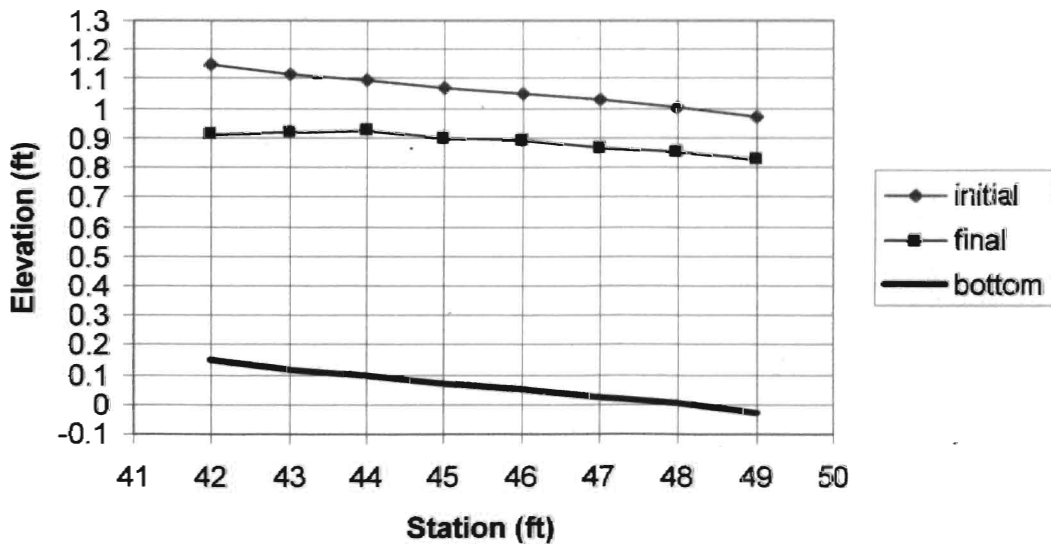
Test No. 3, Bed Profiles for 0.8% Initial Slope
Q = 0.175 cfs and Duration of Test = 18 min
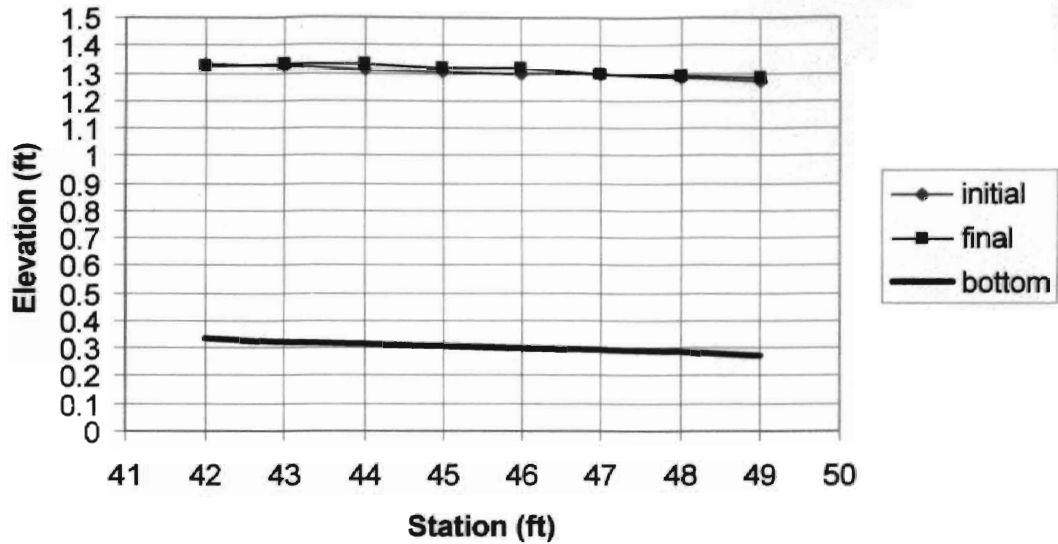
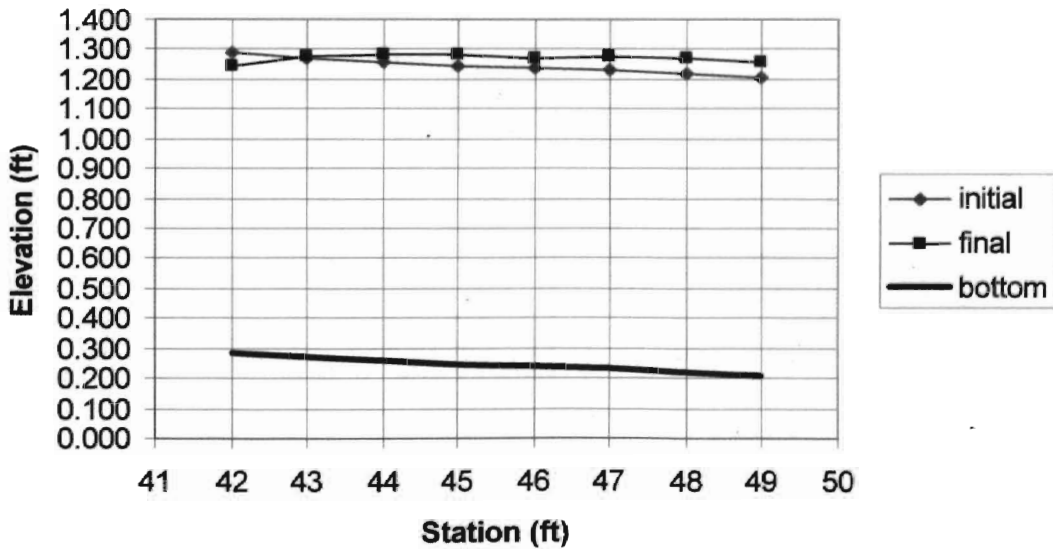Test No. 4, Bed Profiles for 4.5% Initial Slope
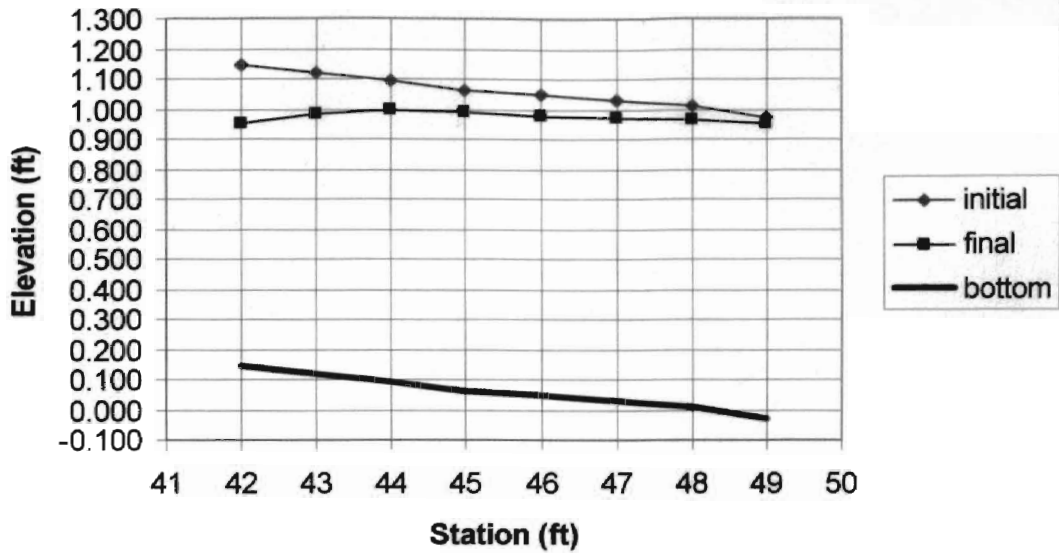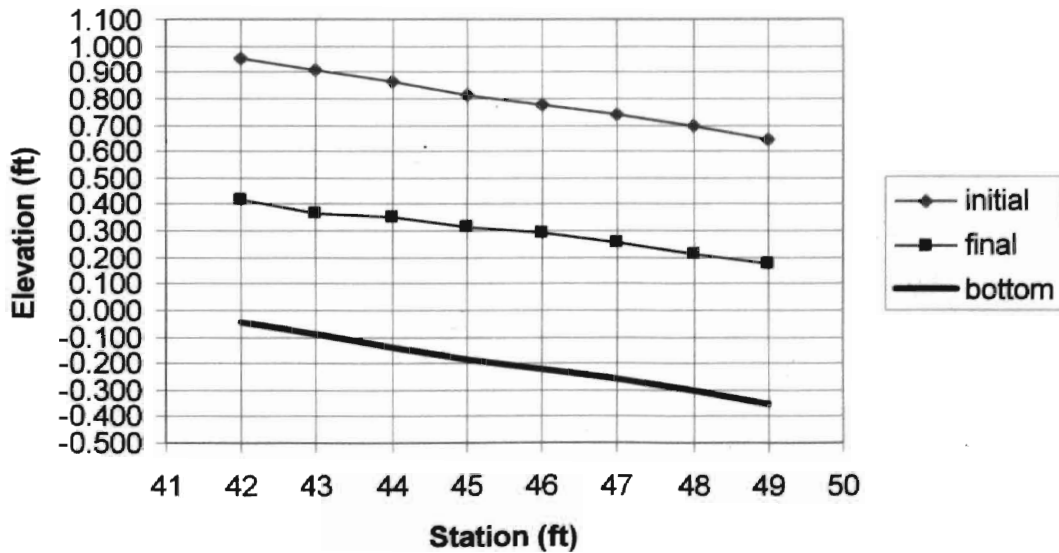Q = 0.175 cfs and Duration of Test = 10 min
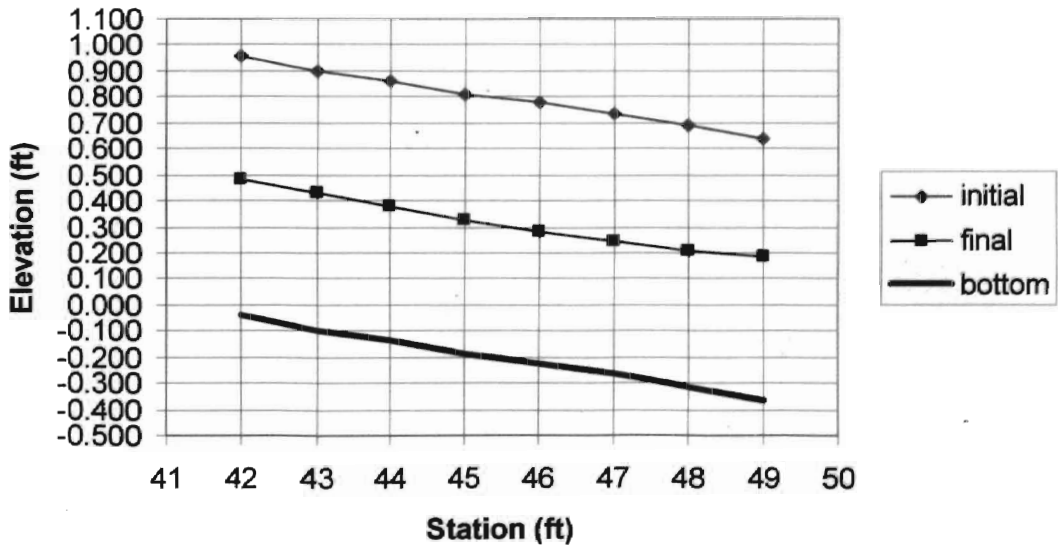
Test No. 5, Bed Profiles for 0.4% Initial Slope
Q = 0.175 cfs and Duration of Test = 19 min

Test No. 6, Bed Profiles for 1.1% Initial Slope
Q = 0.35 cfs and Duration of Test = 23 min

Test No. 7, Bed Profiles for 2.4% Initial Slope
Q = 0.35 cfs and Duration of Test = 15 min

Test No. 8, Bed Profiles for 4.3% Initial Slope
Q = 0.35 cfs and Duration of Test = 10 min

Test No. 9, Bed Profiles for 4.3% Initial Slope
**Q = 0.23 cfs and Duration of Test = 30 min**

Elevation (ft) vs. Station (ft)

Legend: initial, final, bottom
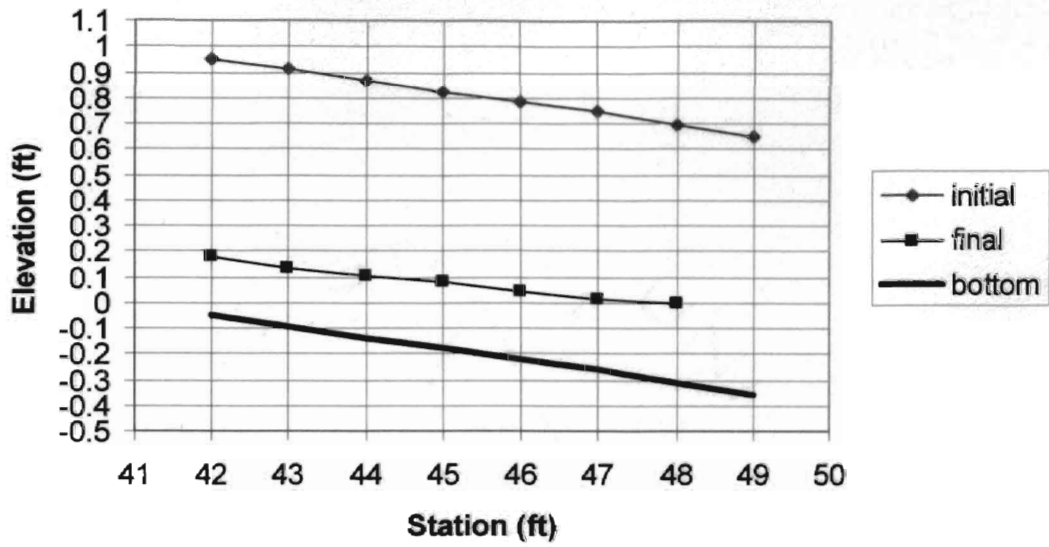
APPENDIX E

Data Analysis for Movable Bed Study

Summary of Results and Data Analysis for Movable-Bed Study

Test (No.)	Slope (%)	Q (cfs)	h (ft)	V (fps)	Q_s (g/sec)	τ (Pa)	T_c (g/sec)	Dr (g/s/m²)	Dc (g/s/m²)	Time (min)	Scour (ft)
1	1	0.170	0.18	1.89	5.0	5.38	82.5	6.5	6.9	73	0.052
2	2.4	0.153	0.11	2.78	77.3	7.89	238.1	84.1	124.5	27	0.176
3	0.8	0.167	0.19	1.76	3.5	4.54	56.2	4.6	4.9	18	-0.009
4	4.5	0.164	0.08	4.10	215.7	10.76	483.4	210.9	380.9	10	0.479
5	0.4	0.171	0.20	1.71	3.3	2.39	13.4	3.8	5.0	19	0.003
6	1.1	0.341	0.20	3.41	4.6	6.57	111.5	6.0	6.3	23	-0.025
7	2.4	0.344	0.18	3.82	95.6	12.91	418.4	111.6	144.6	15	0.086
8	4.3	0.325	0.15	4.33	351.6	19.28	945.1	368.1	586.2	10	0.503
9	4.3	0.225	0.12	3.75	336.9	15.42	738.6	326.2	599.8	30	0.745

APPENDIX F

Sample Images of Flow Profiles

1% Trench Slope

2% Trench Slope

4% Trench Slope
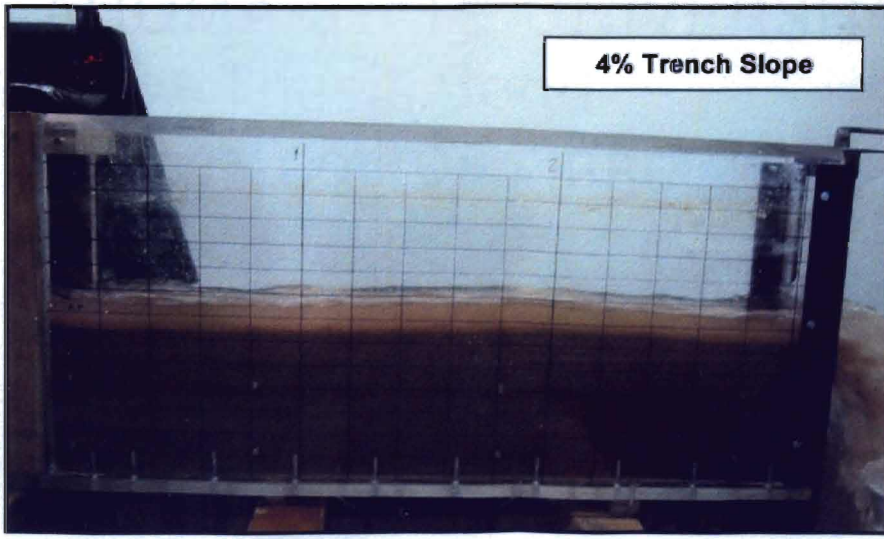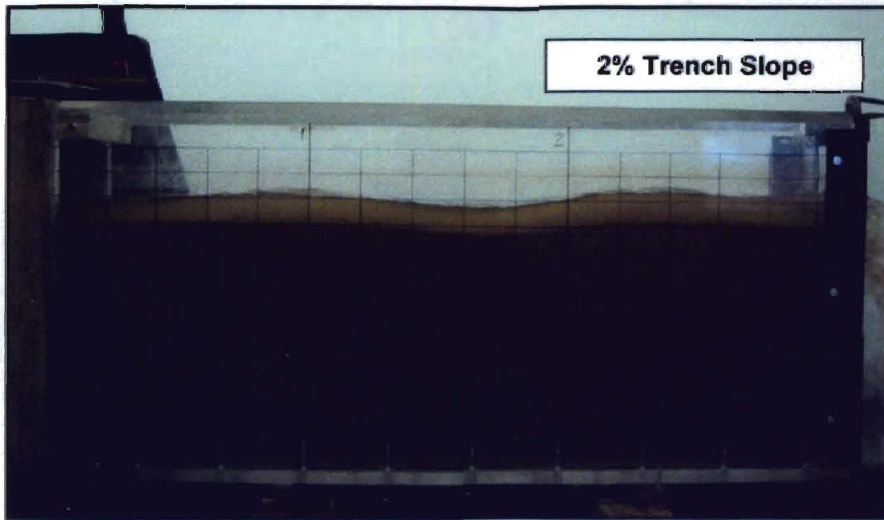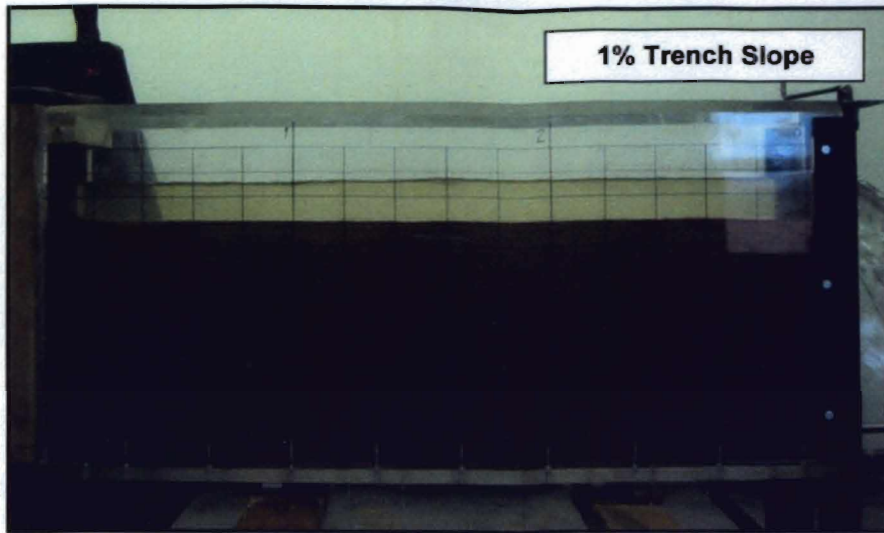
VITA

CHRISTOPHER BRADLEY CROSS

Candidate for the Degree of

Master of Science

Thesis: PERFORMANCE EVALUATION OF SILT FENCE WITH A SLOPING TOE TRENCH

Major Field: Biosystems Engineering

Biographical:

Personal Data: Born in Lawton, Oklahoma on April 26, 1978, the son of Gerald and Charlotte Cross

Education: Received Bachelor of Science degree in Biosystems Engineering at Oklahoma State University, Stillwater, Oklahoma in May 2001; completed the requirements for the Master of Science degree with a major in Biosystems Engineering at Oklahoma State University in August 2003

Professional Experience: Project Engineer for the City of Owasso Department of Public Works, beginning in July 2003; Graduate Research Assistant for the Oklahoma State University Department of Biosystems Engineering, June 2001 to July 2003; Surveyor for Gose and Associates, August 2000 to August 2001; Engineering Aid for the USDA-ARS Hydraulics Engineering Research Laboratory, June 1998 to August 2000

Professional Memberships: Oklahoma State Board of Registration for Professional Engineers and Land Surveyors, Engineering Intern; American Society of Agricultural Engineers; Alpha Epsilon Agricultural Engineering Honor Society; Tau Beta Pi

Scholastic Honors: Phi Kappa Phi National Honor Society and Oklahoma State University College of Engineering Architecture and Technology (CEAT) Scholars Enrichment Program